environments

Article

Ecological and Health Risk Assessment of Total Petroleum Hydrocarbons and Metals in Water Samples from Bille Mangrove, Niger Delta, Nigeria

Onyinyechi G. Opara * and Vsevolod V. Pavshintsev

Institute of Environmental Engineering, Peoples' Friendship University of Russia Named After Patrice Lumumba, 6 Miklukho-Maklaya Street, 117198 Moscow, Russia; pavshintsev-vv@rudn.ru
* Correspondence: onyinyechiopara@yandex.ru

Abstract

Petroleum exploitation in the Niger Delta has caused widespread contamination of mangrove ecosystems, yet studies that integrate total petroleum hydrocarbons (TPH) and metals in mangrove water are still very limited. This study presents the first dual-pollutant baseline assessment of TPH and five priority metals (Cd, Cr, Pb, Ni, Zn) in Bille mangrove water, a severely oil-impacted system supporting about 50,000 residents. Water samples were collected from six sites along a contamination gradient (flow station, pipeline passage, old bunkering site) and analyzed for TPH (C8–C40) and metals. All concentrations are reported in mg/L for direct comparability with World Health Organization (WHO) drinking-water guidelines and United States Environmental Protection Agency (USEPA) thresholds. TPH concentrations ranged from 0.18 to 57.66 mg/L, with Site 3 (pipeline passage) showing levels about 320-fold higher than reference sites and exceeding the WHO drinking-water guideline (0.05 mg/L) by up to 1153-fold. Cadmium (0.040–0.350 mg/L) and nickel (0.055–0.561 mg/L) exceeded WHO drinking-water guidelines (Cd 0.003 mg/L; Ni 0.07 mg/L) by 13–117- and up to 8-fold, respectively. Health risk assessment, using USEPA Risk Assessment Guidance for Superfund (RAGS) protocols, revealed a total cancer risk of 4.15×10^{-3} at Site 3, 41-fold above the USEPA acceptable threshold of 1×10^{-4}, and extreme non-carcinogenic risk (Hazard Index = 20.03–25.51) at petroleum-infrastructure sites; cadmium contributed 86–88% of both carcinogenic and non-carcinogenic effects. Ecological risk indices classified Site 3 as extreme (Potential Ecological Risk Index = 722, against the Håkanson PERI = 600 "very-high-risk" threshold), mainly driven by cadmium (Er = 310–350) and nickel (Er = 140–150). Source apportionment using the Carbon Preference Index, enrichment factors, and strong TPH–metal correlations ($r > 0.88$, $p < 0.01$) clearly identified petroleum operations as the dominant contamination source. This work demonstrates the critical importance of integrated multi-pollutant assessments in petroleum-degraded mangrove water for guiding environmental protection and public-health interventions.

Keywords: mangrove water; total petroleum hydrocarbons (TPH); metals; health risk assessment; ecological risk index; Niger Delta; WHO drinking-water guideline; USEPA cancer risk threshold

Check for updates

Academic Editors: Paloma De Almeida Rodrigues, Adriano Oliveira and Claude Fortin

Received: 9 May 2026
Revised: 13 June 2026
Accepted: 13 June 2026
Published: 24 June 2026

Copyright: © 2026 by the authors. Licensee MDPI, Basel, Switzerland. This article is an open access article distributed under the terms and conditions of the Creative Commons Attribution (CC BY) license.

1. Introduction

1.1. Petroleum Pollution and Mangrove Vulnerability

Mangrove ecosystems, located at the interface between terrestrial petroleum operations and marine environments, represent one of the most vulnerable coastal habitats to hydrocarbon contamination [1,2]. These ecologically vital ecosystems provide essential services including nursery grounds for commercially important fish species, coastal protection, carbon sequestration, and livelihoods for millions of coastal residents [3,4]. Their position in low-energy depositional environments results in the accumulation and long-term retention of persistent organic pollutants and metals, with residence times that extend decades beyond the initial contamination events [5,6]. The anaerobic conditions prevalent in mangrove sediments retard the biodegradation of petroleum hydrocarbons by 50–75% compared with toxic environments [7], while the high lipid content and extensive root systems of mangrove vegetation facilitate bioaccumulation of organic and inorganic contaminants, leading to biomagnification through food webs that directly affect human populations dependent on mangrove-derived protein sources [8,9]. Recent reviews have further documented the cumulative pressures threatening Niger Delta mangroves, including chronic spills, gas flaring, and unregulated artisanal refining [10].

1.2. Total Petroleum Hydrocarbons: Sources, Fate, and Toxicity

Total petroleum hydrocarbons (TPH) encompass a complex mixture of aliphatic and aromatic compounds ranging from C8 to C40+ carbon chains, representing the bulk mass of crude oil contamination in aquatic environments [11,12]. In the Niger Delta, TPH contamination originates from chronic pipeline leaks (estimated at 240,000 barrels annually), operational discharges from flow stations, spills related to sabotage, and artisanal refining activities [13,14]. Recent assessments have documented water TPH concentrations ranging from 17.38 to 889 mg/L in estuarine systems most severely affected [15], exceeding the WHO drinking-water guidelines (0.05 mg/L) by factors greater than 17,000.

The environmental fate of TPH in mangrove systems is governed by competing processes of weathering, biodegradation, photo-oxidation, and sorption to organic-rich sediments [16]. Carbon Preference Index (CPI) and pristane/phytane (Pr/Ph) ratios serve as diagnostic tools to differentiate petrogenic from biogenic sources and to assess weathering status [17,18]. The toxicological effects of TPH are primarily attributed to narcosis rather than to targeted receptor-mediated toxicity [19], although aromatic fractions, particularly BTEX compounds (benzene, toluene, ethylbenzene, xylenes), exhibit specific toxicities that include neurotoxicity and endocrine disruption [20,21]. Importantly, while TPH as a whole mixture lacks established cancer slope factors, the fraction-based risk assessment approach developed by the Total Petroleum Hydrocarbon Criteria Working Group (TPHCWG) enables quantification of non-carcinogenic health risk using fraction-specific reference doses [22]. Recent studies in the Niger Delta have revealed surface sediment TPH concentrations ranging from 129 to 20,600 mg/kg [23], with 54–100% of sampling stations exceeding the EGASPIN intervention value of 5000 mg/kg [24]. The Bodo area in Ogoniland demonstrated surface sediment TPH exceeding 100,000 mg/kg before remediation [25]. Ref. [26] further reported that microbial communities in chronically oiled Niger Delta mangrove sediments display reduced taxonomic diversity, which compromises their natural hydrocarbon-attenuation capacity and reinforces the need for active remediation interventions.

1.3. Metal Co-Contamination in Petroleum Systems

Metal contamination in petroleum-producing regions represents a distinct but interconnected environmental health concern. Priority metals—cadmium (Cd), lead (Pb), chromium (in trivalent Cr(III) and hexavalent Cr(VI) forms), nickel (Ni), zinc (Zn), and copper (Cu)—derive from drilling fluids, produced water, corrosion products, and anti-fouling agents, exhibiting varying degrees of toxicity and bioavailability [27–30]. The hexavalent form Cr(VI) is markedly more soluble, mobile, and toxic than Cr(III) and is classified as a Group 1 human carcinogen by the International Agency for Research on Cancer (IARC); in this study, however, atomic absorption spectrometry quantifies total chromium, and the risk calculations conservatively assume Cr(VI) speciation in line with USEPA RAGS guidance [31–34]. Unlike TPH, several metals possess established carcinogenic potency, with cadmium classified as Group 1 (carcinogenic to humans) and nickel compounds as Group 1 by IARC, while chromium(VI) and lead are classified as Group 1 and Group 2A, respectively [31]. Consequently, in petroleum-impacted systems where metals co-occur with TPH, metals serve as the primary drivers of carcinogenic risk through established cancer slope factors (Cd oral = 6.3; Cr(VI) oral = 0.5; Ni oral = 0.84; Pb oral = 0.0085 per mg/kg/day) [32–35].

Ecological risk assessment employs multiple complementary indices: contamination factor (CF), Geo-accumulation Index (Igeo), Pollution Load Index (PLI), enrichment factor (EF), and the Potential Ecological Risk Index (PERI) developed by Håkanson [36–40]. PERI incorporates metal-specific toxic-response factors that reflect the relative sensitivity of aquatic organisms, with cadmium assigned the highest factor (Tr = 30) among commonly assessed metals and integrated PERI values exceeding 600 indicating very high ecological risk [41–43]. Human health risk assessment quantifies both non-carcinogenic effects (hazard quotient (HQ) and hazard index (HI)) and carcinogenic risks (cancer risk (CR)) for metals with established carcinogenic potency [32,33]. Recent assessments in the mangrove systems of the Niger Delta have revealed HI that exceeds unity in all 113 samples from oil-polluting communities, with infant cancer risks exceeding USEPA thresholds 180 times [44]. In the Isaka–Bundu tidal mangrove swamp, PERI values ranged from 691.94 to 4447, driven primarily by cadmium (Igeo = 4.68–7.71, Class 6: extremely contaminated) [45]. The Nembe mangrove forest similarly exhibited considerable ecological risk (PERI = 309.82) with cadmium contributing ecological risk factors of 186 [46].

1.4. The Niger Delta Context

The Niger Delta, which spans approximately 70,000 km^2 in nine states, represents Africa's largest petroleum-producing region and one of the most severely affected coastal ecosystems in the world [47,48]. Over 66 years of commercial extraction, cumulative production has exceeded 30 billion barrels, while generating an estimated 1.5 million tons of hydrocarbon contamination from approximately 7000 documented spill incidents [49,50], degrading 2370 km^2 of mangrove forests [51]. The UNEP Ogoniland assessment (2011) documented petroleum hydrocarbon contamination in 49% of the sampled wells, with groundwater TPH concentrations 900 times above WHO guidelines and metal contamination across multiple matrices [47,52].

Despite this extensive documentation, no studies have simultaneously assessed TPH and metals in mangrove water samples from the Niger Delta using an integrated risk assessment framework that combines ecological indices with comprehensive human health risk evaluation. Most investigations have focused on single pollutant classes [23,45], have assessed multiple pollutants in sediments rather than in water [25,53], or have examined contamination in terrestrial systems rather than mangrove ecosystems [54].

1.5. Research Gap and Study Objectives

The absence of integrated dual-pollutant assessments of TPH and metals in the mangrove water of the Niger Delta represents a knowledge gap with direct implications for risk management, remediation prioritization, and environmental justice. Single-pollutant assessments fail to capture the interactions between petroleum hydrocarbons and co-occurring metals, misidentify dominant risk drivers, and provide inadequate guidance for resource allocation [55,56]. Dissolved organic matter derived from petroleum hydrocarbon degradation can substantially alter metal speciation, bioavailability, and toxicity through complexation reactions [57,58], making integrated assessment essential. The evaluation of the water column is equally crucial, as water represents the medium of direct exposure to subsistence fishing communities and the vector of transport of contaminants to edible biota [59].

Bille Community, located in Rivers State within the core petroleum zone of the Niger Delta, exemplifies these concerns. The community of approximately 50,000 residents is surrounded by petroleum infrastructure, including flow stations, an extensive pipeline network, and sites of recurring oil spills and illegal bunkering activities [60]. Residents rely heavily on mangrove-derived proteins and have documented health problems, including skin conditions, respiratory diseases, and suspected cancer clusters [61]. The community is engaged in active litigation against petroleum companies, making a comprehensive environmental characterization scientifically and legally imperative.

This study addresses the identified research gap through five specific objectives: (1) quantify concentrations of TPH (C8–C40) and five priority metals (Cd, Cr, Pb, Ni, Zn) in Bille mangrove water across a spatial contamination gradient; (2) characterize spatial distribution patterns and identify primary contamination sources through diagnostic molecular ratios and multivariate statistical analysis; (3) calculate comprehensive ecological risk indices for both pollutant classes; (4) assess human health risks through both carcinogenic (metals) and non-carcinogenic (TPH and metals) pathways; and (5) develop an integrated management framework for evidence-based remediation prioritization specific to Bille Community.

2. Materials and Methods

2.1. Study Area Description

The study was conducted in Bille Community, Rivers State, Niger Delta, Nigeria (4°33′–4°35′ N, 6°53′–6°54′ E). Bille is a coastal mangrove-dominated community with an estimated population of 50,000 residents that depend primarily on fishing, shellfish harvesting, and subsistence agriculture. The area is characterized by extensive mangrove stands of *Rhizophora racemosa* and *Avicennia germinans* interspersed with tidal creeks and channels. Petroleum infrastructure includes multiple flow stations, an extensive pipeline network, historical oil-spill sites, and illegal artisanal-refining sites. The area experiences semi-diurnal tides with a mean range of 1.8–2.4 m and receives a mean annual rainfall of approximately 2500 mm concentrated during the wet season (April–October). The spatial layout of the study area and the six sampling stations is shown in Figure 1.

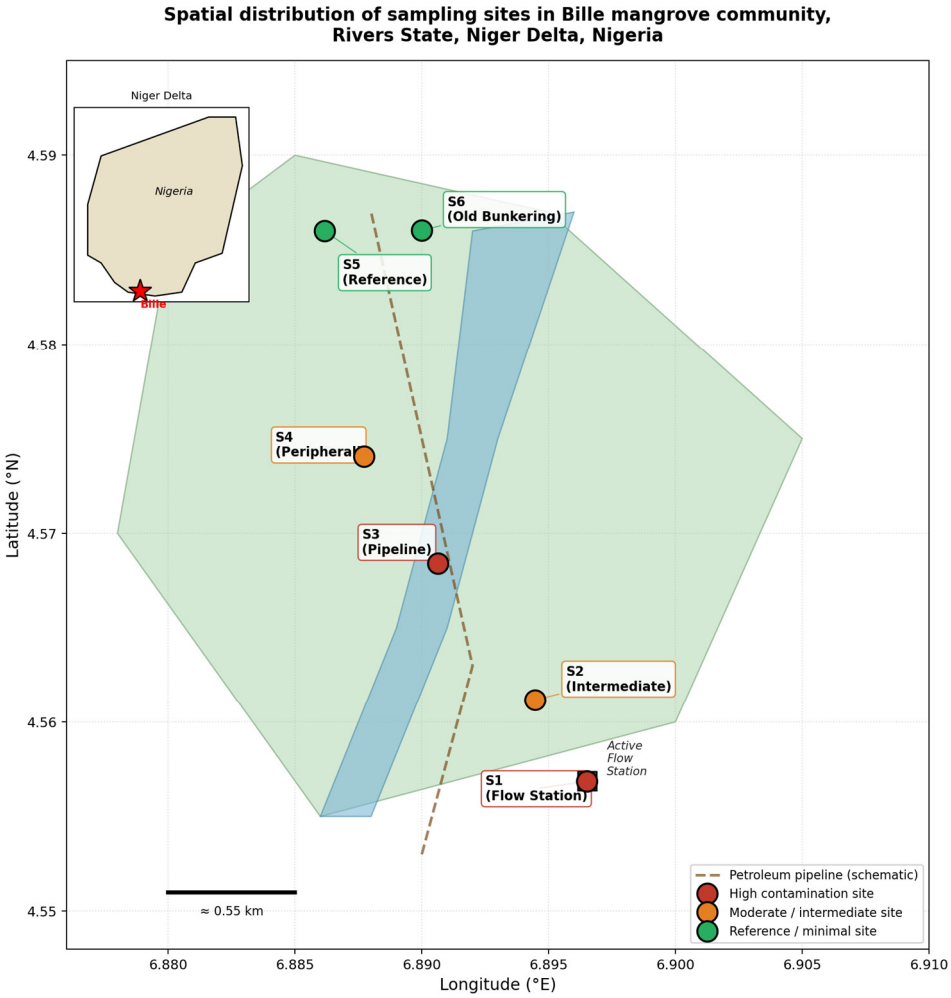


Figure 1. Spatial distribution of the six water-sampling sites in Bille mangrove community, Rivers State, Niger Delta, Nigeria. Sites 1 and 3 (red markers) are located adjacent to active petroleum infrastructure (flow station and buried pipeline). Sites 2 and 4 (orange) are intermediate locations. Sites 5 and 6 (green) are minimally affected reference sites; Site 6 is an old, inactive bunkering location. The schematic creek and mangrove polygons are illustrative; exact site coordinates are listed in Table 1.

Table 1. Sampling-site characteristics in Bille mangrove community. Coordinates were recorded in the field using a handheld GPS receiver (Garmin GPSMAP 64s, Garmin International Inc., Olathe, KS, USA). "Contamination class" refers to the remediation tier defined in Section 4.9. Petroleum infrastructure positions are illustrated schematically in Figure 1.

Site	Coordinates	Description and Proximity to Petroleum Infrastructure	Contamination Class
S1	4°33′24.7″ N 6°53′47.4″ E	Active oil-company flow station with documented spillage history; located within ~200 m of operational separators and produced-water discharge.	High (Tier 1)
S2	4°33′40.3″ N 6°53′40.1″ E	Intermediate location downstream of the flow station, ~500 m from S1 along the principal tidal channel.	Moderate (Tier 2)

Table 1. *Cont.*

Site	Coordinates	Description and Proximity to Petroleum Infrastructure	Contamination Class
S3	4°34′6.3″ N 6°53′26.3″ E	Major petroleum pipeline passage with visible surface soil staining and vegetation mortality; the site overlies a buried 24-inch trunkline.	High (Tier 1)
S4	4°34′26.6″ N 6°53′15.8″ E	Intermediate peripheral location situated between the pipeline corridor and the reference cluster.	Moderate (Tier 2)
S5	4°35′9.6″ N 6°53′10.2″ E	Minimally affected reference site within an undisturbed mangrove fringe; no documented petroleum infrastructure within 1 km.	Reference (Tier 3)
S6	4°35′9.7″ N 6°53′24.0″ E	Old, inactive artisanal bunkering location; site retained as a reference because no fresh hydrocarbon input has been observed for > 5 years.	Reference (Tier 3)

2.2. Sample Site Selection and Collection

Six sampling sites were strategically selected to represent a contamination gradient, ranging from active petroleum infrastructure to minimally affected reference locations (Table 1; Figure 1). Site coordinates and contamination context are summarized in Table 1 for clarity.

Water samples were collected during the dry season (September 2025) at low tide to minimize dilution effects. Triplicate 1-L samples were collected at each site using pre-cleaned amber-glass bottles for organic analysis and acid-washed polyethylene bottles for heavy-metal analysis. Samples for organic analysis were preserved with dichloromethane (5 mL per liter) and refrigerated at 4 °C. Heavy-metal samples were acidified with concentrated HNO_3 (pH < 2) immediately after collection. All samples were transported on ice to the laboratory within 6 h and processed within 48 h.

2.3. Total Petroleum Hydrocarbon (TPH) Analysis

TPH analysis followed USEPA Method 8015C with modifications for complex environmental matrices [62,63]. Water samples (100 mL) were extracted three times with n-hexane (50 mL each), combined, and concentrated to 1 mL using a rotary evaporator (Büchi R-100, Büchi Labortechnik AG, Flawil, Switzerland), then cleaned on activated silica gel (heated at 105 °C for 12 h) and further concentrated to 0.5 mL under a gentle stream of high-purity nitrogen. Gas chromatography with flame-ionization detection was performed on an Agilent 7890B GC-FID (Agilent Technologies Inc., Santa Clara, CA, USA) employing an HP-5MS capillary column (30 m × 0.25 mm i.d. × 0.25 µm film thickness, Agilent J&W, Santa Clara, CA, USA). Operating conditions were injector 280 °C; detector 300 °C; splitless injection (1 µL); oven program 50 °C (hold 2 min) → 15 °C/min to 150 °C → 8 °C/min to 280 °C (hold 10 min); helium carrier at 1.2 mL/min. Quantification was performed using a certified C8–C40 n-alkane mixture (Restek Corporation, Bellefonte, PA, USA) with internal-standard calibration (squalane).

The Carbon Preference Index (CPI), used to discriminate petrogenic and biogenic hydrocarbons [17,18], was calculated as follows:

$$CPI = 0.5 \times [\Sigma C_{25–33}\ (\text{odd})/\Sigma C_{24–32}\ (\text{even}) + \Sigma C_{25–33}\ (\text{odd})/\Sigma C_{26–34}\ (\text{even})] \quad (1)$$

where CPI ≈ 1.0 indicates petroleum origin and CPI > 1.0 suggests biogenic input.

2.4. Metal Analysis

Heavy-metal concentrations (Cd, Cr (total), Pb, Ni, Zn) were determined by atomic absorption spectroscopy (AAS) following APHA Method 3030E [64]. Although Cr(VI) and Cr(III) differ markedly in toxicity, total chromium was quantified by AAS in this study; for the carcinogenic-risk calculation, a conservative Cr(VI) assumption was applied in line with USEPA RAGS guidance [32,34], and this assumption is discussed as a methodological limitation in Section 4.8. Water samples (10 mL aliquots) were digested with 5 mL of concentrated HNO_3 on a hot plate at 95 °C until volume reduced to 5 mL. After cooling, 2 mL of 30% H_2O_2 was added, and heating continued until the digest became clear. The digest was filtered (Whatman 42, Cytiva, Marlborough, MA, USA), diluted to 50 mL with ultrapure water, and analyzed by flame AAS using a PerkinElmer AAnalyst 400 atomic absorption spectrometer (PerkinElmer Inc., Waltham, MA, USA). Operating parameters were Cd (λ = 228.8 nm, slit 0.7 nm); Cr (λ = 357.9 nm, slit 0.7 nm); Pb (λ = 283.3 nm, slit 0.7 nm); Ni (λ = 232.0 nm, slit 0.2 nm); Zn was determined by the cold-vapor-generation accessory of the same instrument. Calibration curves (R^2 > 0.998) were prepared from multi-element CertiPUR reference standards (Merck KGaA, Darmstadt, Germany); all measurements were background-corrected and performed in triplicate.

2.5. Physicochemical Parameters

The physicochemical properties of the water samples were measured in situ and in the laboratory following standard methods [62]. Field measurements of temperature, pH, dissolved oxygen and electrical conductivity. were conducted using a calibrated multiparameter probe (Hanna HI 9829 multiparameter meter, Hanna Instruments Inc., Woonsocket, RI, USA) (see Table 2). Salinity was determined using a handheld refractometer (ATAGO MASTER-S/Millα, ATAGO Co., Ltd., Tokyo, Japan). Laboratory analysis included total dissolved solids (gravimetric, 180 °C; APHA Method 2540C), chemical oxygen demand (APHA Method 5220D), biochemical oxygen demand (APHA Method 5210B), total organic carbon (combustion–infrared detection on a Shimadzu TOC-L analyzer, Shimadzu Corporation, Kyoto, Japan), total organic matter (loss on ignition at 550 °C) (see Table 2), total nitrogen (Kjeldahl digestion, APHA Method 4500-N), phosphorus (ascorbic-acid method, APHA Method 4500-P), and potassium (flame photometry, APHA Method 3500-K).

Table 2. Physicochemical parameters of water samples from the six sites.

Parameter	Unit	S1	S2	S3	S4	S5	S6
Temperature	°C	27.3	27.7	28.3	27.9	28.3	28.6
pH	—	7.73	7.20	7.17	7.38	7.24	7.04
Salinity	ppt	0.98	0.94	0.92	0.82	0.89	0.97
Dissolved oxygen (DO)	mg/L	3.2	4.1	2.8	4.5	5.8	5.6
Electrical conductivity (EC)	µS/cm	1850	1780	1920	1650	1580	1620
Total dissolved solids (TDS)	mg/L	925	890	960	825	790	810
Chemical oxygen demand (COD)	mg/L	48.5	28.3	52.1	22.6	15.2	16.8
Biochemical oxygen demand (BOD)	mg/L	18.2	12.6	20.4	10.8	6.4	7.2
Total organic carbon (TOC)	%	11.25	6.82	9.28	5.14	3.62	3.85
Total organic matter (TOM)	%	19.39	11.75	15.99	8.86	6.24	6.63

Field measurements (temperature, pH, salinity, DO, EC) were performed with a Hanna HI 9829 multiparameter meter (Hanna Instruments, RI, USA) and a refractometer; laboratory analysis followed APHA standard methods [63]. Abbreviations: S1–S6 = sampling sites (see Table 1); DO = dissolved oxygen; EC = electrical conductivity; TDS = total dissolved solids; COD = chemical oxygen demand; BOD = biochemical oxygen demand; TOC = total organic carbon; TOM = total organic matter.

2.6. Quality Assurance and Quality Control

Method blanks (n = 3 per batch) and field blanks (n = 2) were analyzed to assess contamination. Sample duplicates (15% of total) assessed analytical precision. Matrix-spiked samples (10% of total) evaluated method accuracy. Certified reference materials (NIST SRM 1944 and SRM 1640a, National Institute of Standards and Technology, Gaithersburg, MD, USA) were analyzed with each batch. Method detection limits (MDLs) and quantification limits (MQLs) were determined from seven replicate analysis of low-level standards. Calibration curves were verified every10 samples using continuing-calibration-verification standards. Acceptance criteria: blank < MDL; duplicate RPD < 20%; spike recoveries 80–120%; CRM within ±10% of the certified values; CCV within ±15% of the true value. All parameters met the acceptance criteria, confirming the reliability of the data.

2.7. Health and Ecological Risk Assessment Framework

The risk-assessment framework follows the United States Environmental Protection Agency Risk Assessment Guidance for Superfund (RAGS) [32,34] and incorporates the hazard quotient (HQ), hazard index (HI), cancer risk (CR), Potential Ecological Risk Index (PERI), contamination factor (CF), Geo-accumulation Index (Igeo), Pollution Load Index (PLI), and enrichment factor (EF). All formulas, exposure parameters, and toxicological constants are presented explicitly below with their primary literature sources to ensure full methodological transparency.

2.7.1. Chronic Daily Intake (CDI) and Hazard Quotient (HQ)

Chronic daily intake (CDI) was calculated for both pollutant classes following USEPA RAGS [32,34] as follows:

$$CDI = (C \times IR \times EF \times ED)/(BW \times AT) \quad (2)$$

where C is pollutant concentration (mg/L); IR is ingestion rate (2 L/day adults, 1 L/day children) [32]; EF is exposure frequency (350 days/year) [32]; ED is exposure duration (30 years adults, 6 years children) [32,64]; BW is body weight (70 kg adults, 15 kg children) [32]; and AT is averaging time (ED × 365 days for non-cancer; 70 × 365 = 25,550 days for cancer). These default exposure-factor values are taken from the USEPA Exposure Factors Handbook (2011 edition) [64] and are widely used in mangrove-water risk studies in the Niger Delta [44,45,65].

The hazard quotient (HQ) and hazard index (HI) for non-carcinogenic risk were calculated as [32]

$$HQ = CDI/RfD, HI = \Sigma HQ, \quad (3)$$

where RfD is the reference dose. For TPH, the fraction-based approach of the Total Petroleum Hydrocarbon Criteria Working Group (TPHCWG) [22] was applied, with fraction-specific RfDs: aliphatic C > 8–C16 = 0.1 mg/kg/day; aliphatic C > 16–C35 = 2.0 mg/kg/day; aromatic C > 16–C35 = 0.03 mg/kg/day. Reference doses for metals (mg/kg/day) were taken from USEPA IRIS [34] and ATSDR [33]: Cd RfD_ing = 0.001, RfD_derm = 0.00001; Cr(III) RfD_ing = 1.5, RfD_derm = 0.075; Pb RfD_ing = 0.0035; Ni RfD_ing = 0.02, RfD_derm = 0.0054; Zn RfD_ing = 0.3, RfD_derm = 0.06. HQ or HI values below unity indicate an acceptable risk, while values above unity indicate potential adverse effects [32,44].

2.7.2. Heavy-Metal Cancer Risk Calculation Methodology

The carcinogenic risk from metals was calculated as [32,34]

$$CR = CDI \times CSF, \quad (4)$$

where CSF is the cancer slope factor. The cancer slope factors used (per mg/kg/day) were Cd (oral) = 6.3; Cr(VI) (oral) = 0.5; Pb (oral) = 0.0085; Ni (oral) = 0.84. These values are taken from the USEPA Integrated Risk Information System (IRIS) [34] and the California Office of Environmental Health Hazard Assessment Public Health Goals [35], and have been applied in recent Niger Delta water-risk studies [44,45]. The Cd and Ni slope factors are inhalation-derived in IRIS but are applied here to the oral pathway following the regional convention, which is acknowledged as a conservative assumption (see Section 4.8). The total cancer risk was calculated as the sum of the individual metal cancer risks. Risk interpretation: CR < 10^{-6}, negligible; 10^{-6}–10^{-4}, potential concern; >10^{-4}, an unacceptable risk that requires intervention [32]. The carcinogenic risk of the TPH fractions was not assessed because no cancer slope factors have been established for the bulk TPH or its aliphatic fractions by USEPA, ATSDR, or TPHCWG [22,63].

2.7.3. Heavy-Metal Dermal Exposure

Dermal exposure was calculated following USEPA RAGS Part E [32] as

$$CDI_\text{dermal} = (C \times SA \times AF \times ABS \times EF \times ED)/(BW \times AT), \quad (5)$$

where SA is skin surface area (18,000 cm^2 adults, 6600 cm^2 children) [32]; AF is adherence factor (0.07 mg/cm^2) [32]; and ABS is dermal absorption factor (Cd = 0.001; Pb = 0.001; Cr = 0.001; Ni = 0.001; Zn = 0.006) [32,34].

2.7.4. Ecological Risk Indices

Five complementary ecological-risk indices were calculated—the contamination factor (CF) and Contamination Degree (CD) of Håkanson [40], the Geo-accumulation Index (Igeo) of Müller [36], the Pollution Load Index (PLI) of Tomlinson et al. [37], the enrichment factor (EF) [38,39], and the Potential Ecological Risk Index (PERI) [40]—as follows:

$$CF_i = C_\text{metal}/C_\text{background}, \; CD = \Sigma\, CF_i. \quad (6)$$

The Geo-accumulation Index (Igeo), introduced by Müller [36] and widely used in mangrove studies [45,46], quantifies metal contamination relative to the pre-industrial background and is defined as

$$Igeo = log_2\,(C_n/(1.5 \times B_n)), \quad (7)$$

where C_n is the measured concentration of the metal in the sample, B_n is the geochemical background concentration, and 1.5 is the matrix-correction factor introduced by Müller [36] to compensate for natural lithogenic variability. Igeo is interpreted on seven classes [36]: Class 0 (Igeo ≤ 0, unpolluted); Class 1 (0 < Igeo ≤ 1, unpolluted to moderately polluted); Class 2 (1 < Igeo ≤ 2, moderately polluted); Class 3 (2 < Igeo ≤ 3, moderately to strongly polluted); Class 4 (3 < Igeo ≤ 4, strongly polluted); Class 5 (4 < Igeo ≤ 5, strongly to extremely polluted); Class 6 (Igeo > 5, extremely polluted).

The Pollution Load Index (PLI) and enrichment factor (EF) were calculated as [37–39]

$$PLI = (CF_1 \times CF_2 \times \ldots \times CF_n)^{(1/n)}, \; EF = (C_\text{metal}/C_Fe)_\text{sample}/(C_\text{metal}/C_Fe)_\text{background}. \quad (8)$$

Background concentrations used (mg/kg) follow the local Niger Delta crustal averages reported by [45,46]: Cd 0.3; Pb 20; Cr 35; Ni 20; Zn 95. CF classification: <1 low, 1–3 moderate, 3–6 considerable, ≥6 very high. EF classification: <2 minimal, 2–5 moderate, 5–20 significant, 20–40 very high, ≥40 extremely high enrichment [38,39].

The Potential Ecological Risk Index (PERI) of Håkanson [40] was calculated as

$$Er_i = Tr_i \times CF_i, PERI = \Sigma\, Er_i. \quad (9)$$

Toxic-response factors (Tr) follow Håkanson [40]: Cd = 30; Hg = 40; As = 10; Pb = 5; Cu = 5; Ni = 5; Cr = 2; Zn = 1. Single-substance classification: Er < 40 low, 40–80 moderate, 80–160 considerable, 160–320 high, ≥320 very high risk. Integrated PERI classification: <150 low, 150–300 moderate, 300–600 considerable, ≥600 very high risk [40,41].

The above indices are calculation-based screening tools widely adopted in mangrove and freshwater pollution studies [37–46]; they are not substitutes for organism-level ecotoxicological assays. The complementary role of the standardized ISO and OECD microbial-toxicity test battery in confirming ecological risk has recently been reviewed [66]; that battery (e.g., ISO 11348-1:2007 [67] luminescent-bacteria, OECD 209 activated-sludge respiration, OECD 224 anaerobic toxicity) was beyond the scope of the present water-column study but is recommended for future site-confirmation work in Bille (see Section 4.8).

2.8. Source Apportionment

Source differentiation used diagnostic molecular ratios (Table 3). For TPH, CPI values near unity confirmed petroleum origin, while elevated values at reference sites indicated biogenic dominance. Pristane/phytane ratios provided additional confirmation of source character. Heavy-metal enrichment factors (EF > 20 for Cd and Ni) confirmed strong anthropogenic input, corroborated by correlation analysis (TPH–Cd r = 0.88; TPH–Ni r = 0.91; $p < 0.01$) and principal component analysis showing co-loading of TPH and petroleum-associated metals on the same factor.

Table 3. Diagnostic-ratio thresholds for source apportionment of petroleum-derived pollutants. CPI = Carbon Preference Index; Pr/Ph = pristane/phytane ratio; UCM = unresolved complex mixture; EF = enrichment factor; Igeo = geo-accumulation index; PLI = pollution load index. After [17,18,36–40].

Pollutant	Diagnostic Ratio	Threshold	Interpretation
Total Petroleum Hydrocarbons			
	CPI	≈1.0/>1.0	Petroleum/Biogenic
	Pr/Ph	<1.0/>1.0	Anoxic petroleum/Oxic-biodegraded
	Pr/n-C17	<1.0/>1.0	Fresh oil/Biodegraded oil
	UCM/Resolved	>4.0/<4.0	Heavily weathered/Fresh petroleum
Metals			
	EF	<2/2–5/>5	Natural/Moderate anthropogenic/Significant anthropogenic
	Igeo	≤0/0–1/>5	Unpolluted/Low/Extremely polluted
	PLI	<1/>1	Baseline/Progressive deterioration

2.9. Statistical Analysis

Statistical analyses were performed using SPSS Statistics v26 (IBM Corporation, Armonk, NY, USA) and R v4.3.1 (R Foundation for Statistical Computing, Vienna, Austria). Data normality was assessed using the Shapiro–Wilk test. Spatial variability was assessed using one-way ANOVA with a post-hoc Tukey HSD test ($\alpha = 0.05$). Pearson correlation analysis identified relationships between pollutants and physicochemical parameters. Principal Component Analysis (PCA) with varimax rotation identified the major variance-explaining factors. Spatial distribution maps were generated using ArcGIS 10.8 (Esri Inc., Redlands, CA, USA) with Inverse Distance Weighting (IDW) interpolation. Risk calculations used custom R scripts with Monte Carlo simulation (10,000 iterations). Figures were prepared using R ggplot2 and Python 3.13 matplotlib packages.

The integrated dual-pollutant assessment framework, which includes analytical characterization, source apportionment, and dual-track evaluation of human health and ecological risk, is summarized in Figure 2.

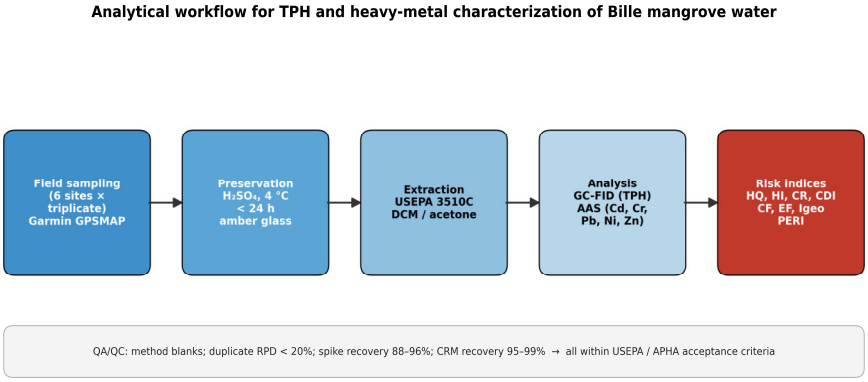


Figure 2. Analytical workflow for TPH and heavy-metal characterization of Bille mangrove water, illustrating the five-phase integrated dual-pollutant assessment framework: field sampling (six sites in triplicate), preservation, extraction (USEPA 3510C), instrumental analysis (GC-FID for TPH, AAS for the priority metals), and downstream risk-index calculation. The QA/QC band below the workflow summarizes the analytical performance metrics achieved across all six sites. Abbreviations: CDI = chronic daily intake; HQ = hazard quotient; HI = hazard index; CR = cancer risk; PERI = Potential Ecological Risk Index; CF = contamination factor; EF = enrichment factor; Igeo = geo-accumulation index; CRM = certified reference material; RPD = relative percent difference; AAS = atomic absorption spectroscopy; GC-FID = gas chromatography with flame-ionization detection; DCM = dichloromethane.

3. Results

3.1. Quality Assurance and Physicochemical Parameters

All quality-assurance/quality-control parameters met the acceptance criteria (Table 4). Method blanks were below the detection limits, duplicate relative percent differences (RPDs) were <20%, spike recoveries ranged from 88% to 96%, and the certified-reference-material (CRM) recovery was within ±10% of the certified values, confirming the reliability of all analytical measurements.

Table 4. Quality-assurance and quality-control summary for all analytical methods. Abbreviations: TPH = total petroleum hydrocarbons; Cd, Cr, Pb, Ni, Zn = cadmium, chromium, lead, nickel, zinc; RPD = relative percent difference; CRM = certified reference material; MDL = method detection limit; MQL = method quantification limit. "<MDL" and "<0.01" entries indicate values below the detection or quantification limit. All parameters fall within the acceptance criteria specified in Section 2.6 (RPD < 20%; spike 80–120%; CRM ± 10%).

Parameter	Method Blank	Duplicate RPD (%)	Spike Recovery (%)	CRM Recovery (%)	MDL (mg/L)	MQL (mg/L)
TPH	<0.01	8.5	92 ± 6	95 ± 4	0.05	0.15
Cd	<MDL	4.2	96 ± 3	98 ± 2	0.001	0.003
Cr	<MDL	5.8	94 ± 4	97 ± 3	0.005	0.015
Pb	<MDL	6.1	91 ± 5	96 ± 3	0.002	0.006
Ni	<MDL	5.3	93 ± 4	97 ± 3	0.003	0.009
Zn	<MDL	3.9	95 ± 3	99 ± 2	0.002	0.006

3.2. Spatial Distribution of Total Petroleum Hydrocarbons

TPH concentrations exhibited pronounced spatial variability, ranging from 0.18 mg/L at the reference sites (S5, S6) to 57.66 mg/L at S3 (pipeline passage) (Table 5). Site 3 demonstrated a 320-fold elevation above the reference sites, implicating the petroleum pipeline as the primary source of contamination. Site 1 (flow station) exhibited the second-highest concentration (30.65 mg/L), representing a 170-fold elevation above baseline. Sites 2 and 4 showed moderate contamination (1.25–1.47 mg/L), while Sites 5 and 6 served as appropriate reference locations.

Table 5. Total petroleum hydrocarbon (TPH) concentrations and diagnostic source-apportionment ratios at six sampling sites. Abbreviations: S1–S6 = sampling sites (see Table 1 for coordinates and contamination context); CPI = Carbon Preference Index; Pr/Ph = pristane/phytane ratio; UCM = unresolved complex mixture. CPI ≈ 1.0 indicates petroleum origin; CPI > 1.0 indicates biogenic input. Pr/Ph < 1 indicates anaerobic/petroleum, Pr/Ph > 1 indicates aerobic/biogenic. EGASPIN sediment intervention value: 5000 mg/kg (applied to sediment, shown here for reference). WHO drinking-water guideline: 0.05 mg/L. Petroleum-impacted sites (S1, S3) exceed the WHO water guideline by 600–1150-fold.

Parameter	S1	S2	S3	S4	S5	S6
TPH (mg/L)	30.65	1.47	57.66	1.25	0.18	0.18
CPI	0.96	1.04	0.98	1.02	1.08	1.12
Pr/Ph	0.92	1.34	0.89	1.28	1.85	1.78
UCM/Resolved	4.8	1.9	5.6	2.1	0.6	0.7
Source (interpreted)	Petroleum	Mixed	Petroleum	Mixed	Biogenic	Biogenic

CPI values at the contaminated sites (0.96–0.98 at S1 and S3) approached unity, confirming an unweathered to moderately weathered petroleum origin. The reference sites exhibited CPI values of 1.08–1.12, indicating biogenic hydrocarbon contributions. The carbon-chain distribution at S1 and S3 was dominated by characteristic n-alkanes of C15–C35 typical of weathered crude oil; the absence of light fractions (C8–C12) at all sites suggests evaporative loss or weathering (see Figure 3).

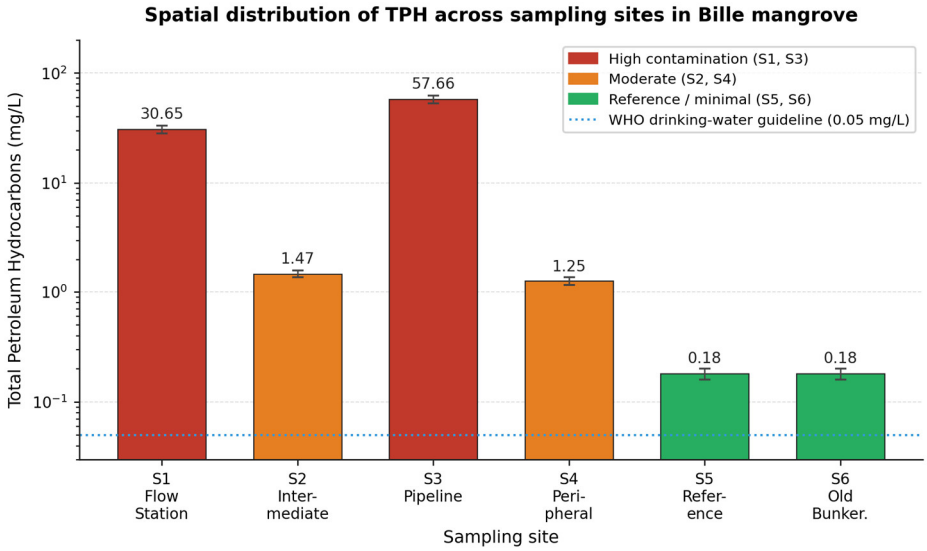


Figure 3. Spatial distribution of total petroleum hydrocarbons (TPH) across six sampling sites in Bille mangrove. Site 3 (pipeline passage) exhibits the highest contamination (57.66 mg/L), a 320-fold elevation above the reference sites (S5 and S6: 0.18 mg/L). Site 1 (flow station) demonstrates the second-highest contamination (30.65 mg/L). The horizontal dotted line indicates the WHO drinking-water guideline (0.05 mg/L). Color coding: red = high contamination (>30 mg/L); orange = moderate (1–30 mg/L); green = reference/baseline (<1 mg/L). Error bars represent the standard deviation of triplicate measurements.

3.3. Heavy-Metal Contamination and Regulatory Exceedances

Heavy-metal concentrations exhibited site-specific patterns with pronounced elevation at petroleum-infrastructure locations (Table 6). Cadmium ranged from 0.040 mg/L (S5) to 0.350 mg/L (S3); S1 and S3 exceeded WHO drinking-water guidelines (0.003 mg/L) by factors of 103–117. Nickel showed the widest range (0.055–0.561 mg/L), with S3 showing a 10-fold elevation above the lowest value and an 8-fold exceedance of the WHO guideline (0.07 mg/L). Lead concentrations (0.010–0.101 mg/L) exceeded WHO guidelines (0.01 mg/L) at S1, S2, and S3 by factors of 6.8–10.1.

Table 6. Heavy-metal concentrations (mg/L) at the six sampling sites compared with WHO drinking-water guidelines and EGASPIN intervention values. Chromium values are reported as total chromium; given the oxidizing estuarine conditions (DO = 2.8–5.8 mg/L; pH 7.04–7.73), a substantial fraction is expected as Cr(VI), the carcinogenic form (IARC Group 1) used in the cancer-risk calculations. Cd, Pb, and Ni at S1 and S3 exceed WHO guidelines by 6–117-fold; Cd at S1 and S3 exceeds the EGASPIN intervention value by 31–35-fold. Reported values are means of triplicate analysis (RSD < 8% for all metals).

Metal	S1	S2	S3	S4	S5	S6	WHO (mg/L)	EGASPIN (mg/L)
Cd	0.310	0.058	0.350	0.051	0.040	0.045	0.003	0.01
Cr (total)	0.123	0.133	0.118	0.176	0.145	0.165	0.05	0.10
Pb	0.068	0.056	0.101	0.021	0.010	0.012	0.01	0.05
Ni	0.301	0.055	0.561	0.120	0.185	0.088	0.07	0.05
Zn	0.057	0.095	0.089	0.013	0.007	0.008	3.00	1.00

Chromium showed a relatively uniform distribution across all sites (0.118–0.176 mg/L), exceeding WHO guidelines by 2.4–3.5 times, suggesting diffuse anthropogenic input from atmospheric deposition or background geological contribution rather than the point-source character of cadmium and nickel. Zinc concentrations (0.007–0.095 mg/L) remained well below the WHO guideline (3.0 mg/L). Figure 4 illustrates the consistent contamination hi-

erarchy in which S3 registered the highest concentrations across all five metals, followed by S1, with a progressive decline toward the reference locations. This spatial gradient mirrors the TPH distribution, and the concordance between the two independent pollutant classes constitutes strong geochemical evidence that petroleum infrastructure—specifically, the pipeline at S3 and the flow station at S1—serves as the unified source of both hydrocarbon and heavy-metal contamination.

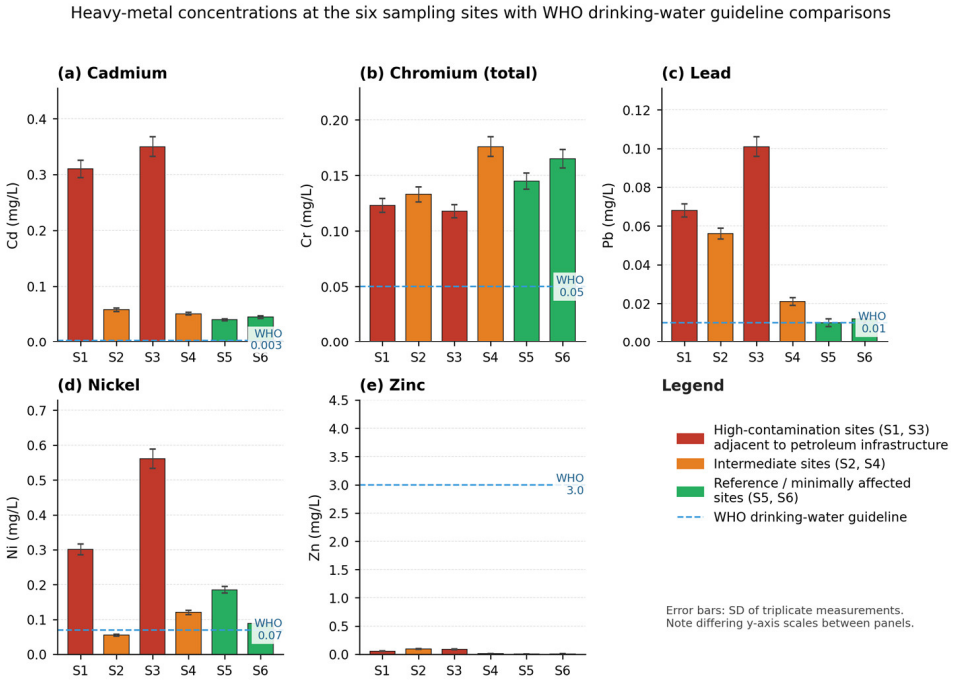


Figure 4. Five-panel heavy-metal distribution across the six sampling sites with WHO drinking-water-guideline comparisons. Panel (**a**) cadmium: S3 shows the highest concentration (0.350 mg/L), 117-fold above the WHO guideline (0.003 mg/L; dashed line). Panel (**b**) chromium: ubiquitous elevation (0.118–0.176 mg/L), 2.4–3.5-fold above the WHO guideline (0.05 mg/L), suggesting diffuse anthropogenic input. Panel (**c**) lead: S1–S3 exceed the WHO guideline (0.01 mg/L) by 6.8–10.1-fold. Panel (**d**) nickel: S3 shows the highest concentration (0.561 mg/L), 8-fold above the WHO guideline (0.07 mg/L). Panel (**e**) zinc: all sites remain within acceptable limits (<3.0 mg/L WHO guideline). Error bars represent the standard deviation of triplicate measurements.

3.4. Heavy-Metal Cancer Risk Assessment

The cancer risk from metals exceeded acceptable thresholds at the petroleum-infrastructure sites (Table 7). Cadmium dominated metal carcinogenic risk, contributing 86–88% of total metal cancer risk across all sites. Site 3 exhibited the highest cancer risk (4.15×10^{-3}), driven primarily by cadmium (3.33×10^{-3}) and nickel (7.12×10^{-4}). Site 1 demonstrated a similarly elevated risk (3.43×10^{-3}). Even the reference sites exhibited detectable metal cancer risk ($6.68–7.29 \times 10^{-4}$), exceeding the USEPA acceptable threshold of 1×10^{-4} by 6.7–7.3-fold, indicating that background heavy-metal contamination in the petroleum-producing region poses baseline carcinogenic concern. For approximately 50,000 residents of Bille Community, continued exposure at current levels at S1 and S3 translates to a probability of cancer of 0.34–0.42%, substantially above acceptable levels (Figure 5).

Table 7. Heavy-metal cancer risk (CR, lifetime probability) by metal and by site, computed from Equation (4) using oral cancer slope factors (CSFs) from the USEPA IRIS database [68] and California OEHHA [64]: Cd 6.3, Cr(VI) 0.5, Pb 0.0085, Ni 0.84 $(mg/kg/day)^{-1}$. CR values $\geq 1 \times 10^{-4}$ are above the USEPA acceptable threshold. Cadmium contributes 86–88% of total metal cancer risk across all sites. Sites 1 and 3 exceed the USEPA threshold by 34–41-fold, indicating an unacceptable carcinogenic risk requiring immediate intervention.

Metal	CSF $(mg/kg/day)^{-1}$	S1	S2	S3	S4	S5	S6
Cd	6.3	2.80×10^{-3}	5.24×10^{-4}	3.33×10^{-3}	4.60×10^{-4}	3.61×10^{-4}	4.06×10^{-4}
Cr(VI)	0.5	8.81×10^{-5}	9.52×10^{-5}	8.45×10^{-5}	1.26×10^{-4}	1.04×10^{-4}	1.18×10^{-4}
Pb	0.0085	8.28×10^{-6}	6.82×10^{-6}	1.23×10^{-5}	2.56×10^{-6}	1.22×10^{-6}	1.46×10^{-6}
Ni	0.84	3.62×10^{-4}	6.62×10^{-5}	7.12×10^{-4}	1.44×10^{-4}	2.22×10^{-4}	1.06×10^{-4}
Total CR	—	$\mathbf{3.43 \times 10^{-3}}$	$\mathbf{7.26 \times 10^{-4}}$	$\mathbf{4.15 \times 10^{-3}}$	$\mathbf{7.71 \times 10^{-4}}$	$\mathbf{7.29 \times 10^{-4}}$	$\mathbf{6.68 \times 10^{-4}}$

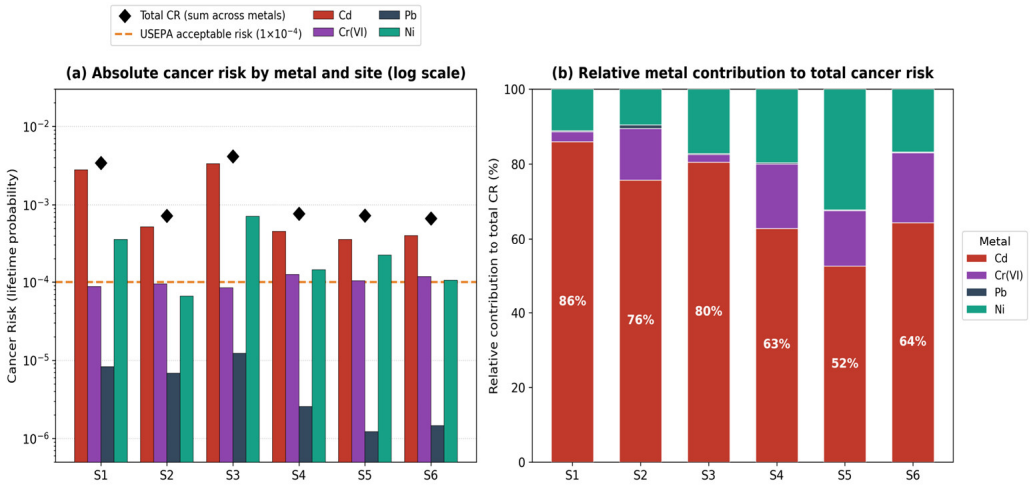


Figure 5. Heavy-metal cancer-risk assessment across the six sampling sites. Panel (**a**): Absolute cancer risk (CR) on a logarithmic scale, showing CR for individual metals (Cd, Cr(VI), Ni, Pb) and total metal CR (black diamonds) at each site. Sites 1 and 3 exhibit the highest total CR (3.43×10^{-3} and 4.15×10^{-3}, respectively). The orange dashed line indicates the USEPA acceptable threshold (1×10^{-4}). Panel (**b**): Relative contribution analysis demonstrating cadmium dominance, contributing approximately 52–86% of total metal cancer risk across all sites, followed by nickel (10–47%),chromium ($\leq$1.5%), and lead (<1%). All sites exceed the USEPA acceptable threshold, with S1 and S3 exceeding it by 34- to 41-fold.

3.5. Non-Carcinogenic Health Risk

Metals dominated the non-carcinogenic health risk, with HI values exceeding unity at all six sites (Table 8). S1 and S3 exhibited extreme non-cancer risk (HI = 20.03 and 25.51), indicating the potential for adverse health effects 20–25 times above acceptable thresholds. Even the reference sites showed HI of 3.90–4.43, confirming that baseline metal contamination throughout the petroleum-producing region poses non-carcinogenic health concern. Cadmium contributed the largest proportion (HQ = 0.60–5.28; 23–37% of total HI), followed by lead (HQ = 0.43–4.36; 14–29%) and nickel (HQ = 0.66–4.23; 12–23%). Dermal and ingestion pathways contributed approximately equally for cadmium and lead, while ingestion dominated for nickel. The cumulative burden indicates probable adverse health effects at S1–S4, with potential manifestations including renal toxicity, neurotoxicity, dermatitis, and respiratory effects [31–33,44].

Table 8. Heavy-metal non-carcinogenic risk expressed as hazard quotient (HQ) per metal and exposure pathway and as hazard index (HI, sum of HQ) per site. Computed using Equations (3), (5), and (6) with oral reference doses (RfDs) from USEPA IRIS [69]: Cd 5×10^{-4}, Cr(VI) 3×10^{-3}, Pb 1.4×10^{-3}, Ni 2×10^{-2}, Zn 0.3 (mg/kg/day); dermal RfD = $RfD_{oral} \times$ GI absorption factor. HI > 1 indicates the potential for non-carcinogenic adverse health effects.

Metal	Pathway	S1	S2	S3	S4	S5	S6
Cd	ingestion	4.68	0.88	5.28	0.77	0.60	0.68
Cd	dermal	4.68	0.88	5.28	0.77	0.60	0.68
Cr (VI)	ingestion	0.13	0.13	0.12	0.18	0.15	0.17
Cr (VI)	dermal	0.25	0.27	0.24	0.35	0.30	0.33
Pb	ingestion	3.58	2.93	4.36	1.34	0.43	0.56
Pb	dermal	3.58	2.93	4.36	1.34	0.43	0.56
Ni	ingestion	2.27	0.42	4.23	0.91	1.40	0.66
Ni	dermal	0.84	0.15	1.57	0.34	0.52	0.25
Zn	ingestion	0.03	0.05	0.05	0.01	0.01	0.01
Zn	dermal	0.01	0.02	0.02	<0.01	0.01	0.01
HI (total)	—	**20.03**	**8.68**	**25.51**	**6.01**	**4.43**	**3.90**

TPH contributed supplementary non-carcinogenic risk through the TPHCWG fraction-based assessment. At the concentrations observed in Bille mangrove water, however, the HQ attributable to TPH remained below unity at all sites, consistent with Ihunwo et al. [65], who reported water-pathway TPH HI of 10^{-5} to 10^{-4} even in contaminated creeks of the Niger Delta. The dominance of metals in non-carcinogenic risk (HI = 20–25) relative to the minimal contribution of TPH confirms that metal remediation must be the primary target for reducing non-cancer health risks.

3.6. Comprehensive Ecological Risk Assessment

PERI calculations revealed very high to extreme ecological risk at petroleum-impacted sites, with values reaching 722 at S3 (Table 9), exceeding the Håkanson "very-high-risk" threshold (PERI $\geq$ 600) by a factor of 1.2. Site 1 demonstrated comparable ecological risk (PERI = 603). Cadmium dominated total ecological risk with individual Er values of 310–350 at S1 and S3, classified as "very high" single-substance risk (Er $\geq$ 320). Nickel contributed the second-highest ecological risk (Er = 75–140), classified as "moderate" to "considerable" risk. Sites 2 and 4 exhibited PERI values of 121–134, classified as low ecological risk, while the reference sites showed PERI of 109–125.

EF analysis confirmed strong anthropogenic sources, with cadmium (EF = 28.6–32.3) and nickel (EF = 41.7–77.6) classified as "very high" to "extremely high" enrichment. Nickel's EF of 77.6 at S3 is among the highest globally for petroleum-impacted systems. Igeo classifications corroborated severe contamination, with S3 cadmium (Igeo = 3.13, Class 3: moderate to strongly polluted) and nickel (Igeo = 4.39, Class 4: strongly polluted), indicating progressive accumulation beyond natural background. The reference sites demonstrated a baseline metal PERI of 109–125, indicating that even minimally affected locations within the petroleum-producing region experience metal enrichment above background, likely from atmospheric deposition of combustion products. The comprehensive ecological-risk assessment is presented graphically in Figure 6.

Table 9. Comprehensive ecological-risk indices for metals at the six sampling sites. Indices and equations: CF (contamination factor, Equation (6)) [39]; CD (sum of CFs); PLI (Pollution Load Index, Equation (8)) [40]; Igeo (Geo-accumulation Index, Equation (7)) [37]; EF (enrichment factor, Equation (8)) [38]; Er (individual potential ecological risk, Equation (9)) [41]; PERI (Potential Ecological Risk Index, Equation (9)) [41]. Classification thresholds (Håkanson [41]): PERI < 150 = low; 150–300 = moderate; 300–600 = considerable; ≥600 = very high. Cadmium dominates ecological risk at S1 and S3 (Er ≥ 320 = very high single-substance risk).

Index	S1	S2	S3	S4	S5	S6
CF (Cd)	10.33	1.93	11.67	1.70	1.33	1.50
CF (Ni)	15.05	2.75	28.05	6.00	9.25	4.40
CF (Pb)	3.40	2.80	5.05	1.05	0.50	0.60
CF (Cr)	3.51	3.80	3.37	5.03	4.14	4.71
CF (Zn)	0.60	1.00	0.94	0.14	0.07	0.08
CD (total)	33.64	12.88	49.14	14.51	15.38	11.37
PLI	4.20	2.45	5.85	2.12	1.74	1.58
Igeo (Cd)	2.95	0.37	3.13	0.26	−0.16	0.09
Igeo (Ni)	3.49	0.96	4.39	2.00	2.79	1.72
EF (Cd)	28.6	5.3	32.3	4.7	3.7	4.2
EF (Ni)	41.7	7.6	77.6	16.6	25.6	12.2
Er (Cd)	310	58	350	51	40	45
Er (Ni)	75	14	140	30	46	22
Er (Pb)	17	14	25	5	3	3
Er (Cr)	7	8	7	10	8	9
Er (Zn)	1	1	1	<1	<1	<1
PERI (Total)	**603**	**121**	**722**	**134**	**125**	**109**
Risk class	**Very high**	**Low**	**Very high**	**Low**	**Low**	**Low**
Risk ranking	**2**	**4**	**1 (WORST)**	**3**	**5**	**6**

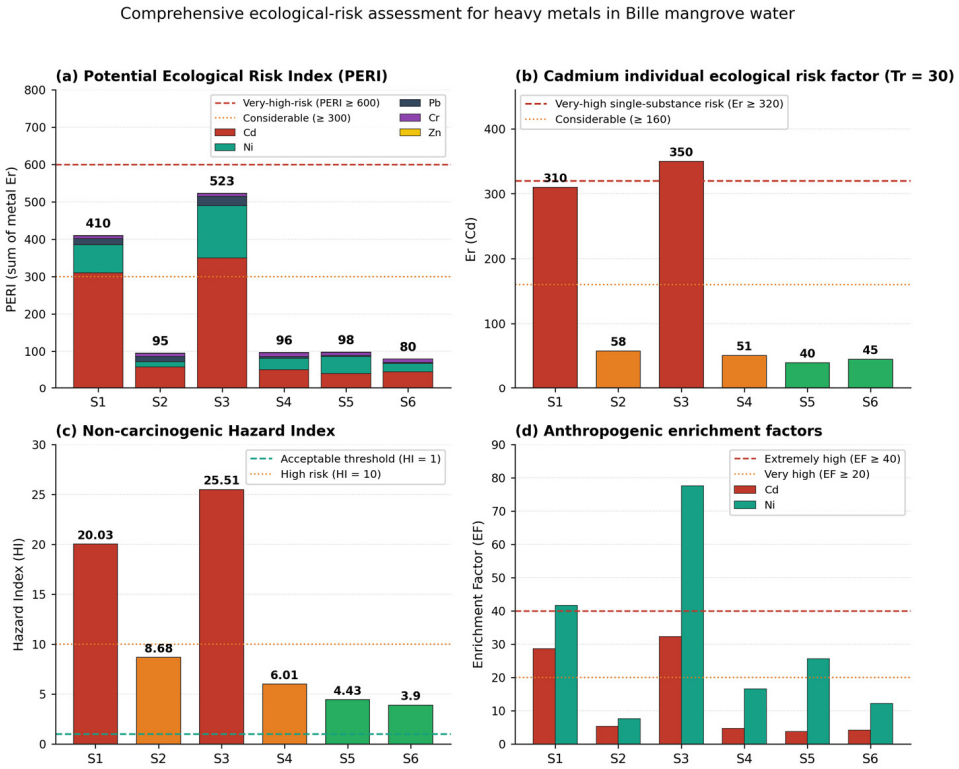


Figure 6. Four-panel comprehensive ecological-risk assessment for metals. Panel (**a**): Heavy-metal Potential Ecological Risk Index (PERI) by site showing stacked contributions from individual metals;

S1 and S3 approach or exceed the "very high risk" threshold (PERI ≥ 600, red dashed line) [40]. Panel (**b**): Individual cadmium ecological risk factor (Er) demonstrating "very high" single-substance risk (Er ≥ 320) at S1 and S3, driven by cadmium's toxic-response factor (Tr = 30). Panel (**c**): Non-carcinogenic hazard index (HI) showing 20–25-fold exceedance of the acceptable threshold (HI = 1, green dashed line) at S1 and S3, driven by cadmium, lead, and nickel. Panel (**d**): Anthropogenic enrichment factors for cadmium and nickel; nickel EF = 77.6 at S3 is classified "extremely high" (≥40) and cadmium EF = 32.3 is "very high" (20–40).

3.7. Source-Apportionment Correlation Analysis

The unified petroleum-infrastructure source of both TPH and heavy-metal contamination is most directly confirmed by Pearson correlation analysis (Figure 7). Strong positive correlations were observed between TPH and the three petroleum-associated metals: TPH–Ni (r = 0.91, $p < 0.01$), TPH–Cd (r = 0.88, $p < 0.01$) and TPH–Pb (r = 0.82, $p < 0.01$). The internal heavy-metal correlation Cd–Ni (r = 0.94) is even stronger, indicating a near-identical spatial pattern of cadmium and nickel that is most parsimoniously explained by their common origin in produced water and corrosion products at the flow station (S1) and pipeline (S3). Chromium uniquely exhibits a weak negative correlation with TPH (r = −0.41) and with the other petroleum-associated metals, consistent with the spatial pattern in Figure 4b and Table 6, in which chromium peaks at the moderate (S4) and reference (S6) sites rather than at S1 and S3. This contrast supports the interpretation that chromium is largely lithogenic/atmospherically deposited at this site and is not delivered by the same point-source pathway as Cd, Ni, and Pb. The correlation results are concordant with those of Anyanwu et al. [15] for the Bonny Estuary and Chris et al. [45] for the Isaka-Bundu mangrove, both of whom reported TPH–metal correlations in the 0.78–0.93 range for cadmium, nickel, and lead in Niger Delta petroleum-impacted systems.

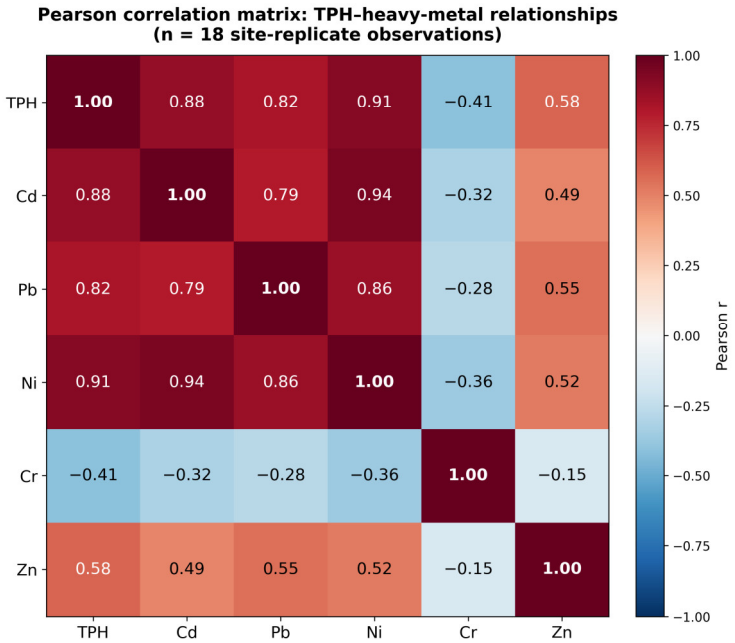


Figure 7. Pearson correlation matrix for TPH and the five priority metals across all eighteen site-replicate observations (six sites × three replicates). Red shading indicates positive correlation; blue shading indicates negative correlation; cell labels report the Pearson r. The strong positive correlations among TPH, Cd, Ni, and Pb (r > 0.79) reflect their common origin in petroleum infrastructure (flow station and pipeline). The weak negative correlation of Cr with TPH and with the other petroleum-associated metals indicates a distinct, diffuse anthropogenic source (likely atmospheric deposition or lithogenic background) rather than the point-source pathway driving Cd, Ni, and Pb.

4. Discussion

4.1. Total Petroleum Hydrocarbons in Regional and Global Context

The TPH concentrations in Bille mangrove water (0.18–57.66 mg/L) occupy an intermediate position within the Niger Delta contamination spectrum, substantially lower than the extreme cases documented by Anyanwu et al. [15] in Bonny Estuary (up to 889 mg/L) and Gundlach et al. [23] at 620 mg/L, yet exceeding WHO drinking-water guidelines by factors of 3.6 to 1153 at contaminated sites. The 320-fold elevation at S3 relative to reference sites, combined with CPI values near unity (0.96–0.98), conclusively demonstrates unweathered to moderately weathered petroleum input at infrastructure locations. The relatively low contamination at S6 (old bunkering site) suggests that artisanal refining has ceased and natural attenuation has reduced residual hydrocarbons to near-background levels. Little et al. [25] documented post-remediation Bodo sediment TPH of 3000–5000 mg/kg, highlighting the intractability of petroleum contamination in mangrove systems even after intensive intervention.

The contribution of TPH to non-carcinogenic risk through the TPHCWG fraction-based approach was minimal in the water pathway, consistent with the findings of Ihunwo et al. [65] in Woji Creek. This reflects the relatively lower bioavailability of petroleum hydrocarbons in the dissolved phase compared with sediment-bound fractions as well as the comparatively higher reference doses established for aliphatic TPH fractions (0.1–2.0 mg/kg/day) relative to heavy-metal RfDs (0.001–0.02 mg/kg/day). Nevertheless, elevated TPH concentrations serve as critical indicators of the petroleum-contamination source and co-occur with metals that drive both carcinogenic and non-carcinogenic risk, making TPH monitoring essential for comprehensive site characterization.

4.2. Heavy-Metal Contamination: Dominant Health and Ecological Risk Driver

Heavy-metal contamination emerges as the dominant risk driver in Bille mangrove across all assessment dimensions. The carcinogenic risk from metals alone ($3.43–4.15 \times 10^{-3}$ at S1 and S3) exceeds the USEPA acceptable threshold (1×10^{-4}) by 34–41-fold, driven primarily by cadmium, which contributes 86–88% of total metal cancer risk. These values are consistent with recent findings by [44] in petroleum-impacted Niger Delta communities, where mean cancer risk exceeded 10^{-4} in all 113 water samples. The Bille values are particularly concerning because they derive from direct water-column exposure in a community reliant on mangrove water for daily activities.

Cadmium emerges as the metal of greatest concern across multiple risk metrics: CF values of 10.33–11.67, regulatory exceedance of 103–117 times WHO guidelines, non-cancer HQ of 4.68–5.28, and 86–88% contribution to total metal cancer risk. Extreme cadmium enrichment (EF = 28.6–32.3) demonstrates anthropogenic origin, with sources including drilling-fluid additives, produced water, and corrosion products from cadmium-plated equipment. The cadmium EF values documented here are consistent with those reported in other petroleum-affected mangrove systems in the Niger Delta, where cadmium typically exhibits the highest enrichment among the assessed metals [45,46,70].

Nickel exhibits the second-highest ecological risk, with CF up to 28.05, Igeo = 3.49–4.39 (Class 4: highly polluted), EF = 41.7–77.6, and FEPA-guideline exceedance up to 28-fold. The EF of 77.6 at S3 ranks among the highest nickel enrichment factors reported worldwide for petroleum-impacted systems. Lead and chromium, while at lower relative enrichments, nevertheless exceed drinking-water guidelines at multiple sites; the uniform chromium distribution suggests diffuse anthropogenic input distinct from the point-source character of cadmium and nickel.

The non-carcinogenic risk profile is equally alarming, with HI values of 20.03–25.51 at S1 and S3 exceeding the acceptable threshold by 20–25-fold. This level of non-carcinogenic

risk indicates that multiple adverse health effects are virtually certain among chronically exposed populations, including renal-tubular dysfunction from cadmium [29,31], neurodevelopmental impairment from lead [31,33], dermatological and respiratory effects from nickel [29,31], and potential endocrine disruption from chromium exposure [31].

4.3. Methodological Basis of the Ecological- and Health-Risk Indices Used

The ecological risk reported here is calculation-based, in line with the screening-level framework of Håkanson [40], Müller [36], and Tomlinson et al. [37]. These indices integrate measured contaminant concentrations with metal-specific toxic-response factors (Tr), and they are widely accepted in the mangrove and freshwater pollution literature [41–46] precisely because organism-level ecotoxicological testing for every site is logistically prohibitive in remote Niger Delta locations.

The toxic-response factors used in PERI (Cd = 30; Hg = 40; As = 10; Pb = 5; Cu = 5; Ni = 5; Cr = 2; Zn = 1) were derived empirically by Håkanson [40] from a combination of bioavailability data, abundance/concentration ratios, and observed biotic effects in aquatic systems. The cadmium factor of 30 reflects its extreme toxicity to aquatic organisms relative to less toxic metals such as zinc [40,41]. The matrix-correction factor of 1.5 in the Igeo formula (Equation (7)) likewise originates from Müller's empirical observation [36] that natural lithogenic variability can introduce up to a 1.5-fold fluctuation in background metal concentrations, and the factor minimizes false-positive contamination classifications.

For human-health risk, the hazard quotient (HQ) and cancer risk (CR) metrics follow the USEPA Risk Assessment Guidance for Superfund (RAGS) [32] and rely on reference doses (RfDs) and cancer slope factors (CSFs) derived from controlled toxicological studies compiled in USEPA IRIS [34] and ATSDR Toxicological Profiles [33]. The RfD framework implicitly incorporates inter- and intra-species uncertainty factors (typically, 100–1000-fold), making HQ a conservative screening metric. The cancer slope factors used here for Cd (6.3), Cr(VI) (0.5), Pb (0.0085), and Ni (0.84) per mg/kg/day are taken from the IRIS database [34] with cross-confirmation from California OEHHA Public Health Goals [35]. Dermal-exposure calculations follow USEPA RAGS Part E [32], using species-specific dermal-absorption factors derived from in vivo and in vitro percutaneous penetration studies. These methodological choices align with all recent Niger Delta water-risk studies [44,45,65].

While calculation-based indices provide essential first-tier risk characterization, organism-level confirmation is desirable for sites flagged as Tier 1 by these indices. The standardized microbial toxicity test battery reviewed by [66]—including the ISO 11348 ("Vibrio fischeri" bioluminescence inhibition), OECD 209 (activated-sludge respiration inhibition), OECD 224 (anaerobic toxicity), OECD 244 (denitrification inhibition), and the more recent enzymatic and gene-expression-based tests—offers a complementary, cost-effective avenue for confirming the ecological hazard of the high-PERI sites identified here (S1 and S3). We therefore explicitly recommend their applications in the follow-up site investigation proposed in Section 4.9 (Tier 1 confirmation work) and in Section 4.8 as a study limitation.

4.4. Comparative Dual-Pollutant Risk Ranking

The integrated dual-pollutant assessment enables quantitative ranking of risk drivers across TPH and heavy-metal classes. For carcinogenic risk, metals are the sole contributor, because TPH as a whole mixture lacks cancer slope factors, and BTEX compounds were not separately quantified in this study. Cadmium alone drives 86–88% of total carcinogenic risk, followed by nickel (7–12%) and chromium (<2%). For non-carcinogenic risk, metals dominate overwhelmingly (HI = 20–25 at petroleum-infrastructure sites), while the contribution of TPH through fraction-based evaluation remains negligible in the water pathway.

For ecological risk, heavy-metal PERI values of 603–722 at S1 and S3 classify these locations as "very high" ecological risk, driven by cadmium's toxic-response factor of 30 and its extreme contamination factors.

This ranking demonstrates that remediation strategies in Bille must prioritize heavy-metal reduction for both health-risk mitigation and ecological recovery, with particular emphasis on cadmium and nickel sources. TPH remediation, while essential for ecosystem restoration and for eliminating the contamination source that delivers co-occurring metals, does not independently drive the risk profile. This finding is consistent with the broader Niger Delta literature in which metals consistently dominate carcinogenic-risk assessments of water resources [44,45].

4.5. Synergistic Effects and Cumulative Risk

The co-occurrence of TPH and metals creates the potential for synergistic toxicological interactions that are not captured by additive risk models. Dissolved organic matter from TPH degradation can complex with metals, altering speciation and bioavailability, as suggested by the elevated TOC (9.28–11.25%) at S1 and S3. The effect of petroleum-derived DOM on metal bioavailability is bidirectional: high-molecular-weight humic-like fractions may sequester free metal ions and reduce acute toxicity, while low-molecular-weight organic acids produced during biodegradation can form soluble metal–organic complexes that enhance dissolved metal concentrations and mobility [57]. Ref. [58] demonstrated that co-contamination with TPH and metals significantly elevated toxicity in bioassays, with lead showing the strongest correlation with toxicity (r = 0.893) under co-contamination conditions.

In mangrove environments, the dynamics of this interaction are particularly complex due to tidal cycling, which creates alternating redox conditions. Petroleum contamination intensifies these cycles by consuming oxygen during biodegradation, reducing redox potential, and stimulating sulfate-reducing bacteria. Under reducing conditions, metal sulfide precipitation (CdS, PbS) temporarily immobilizes metals, but subsequent tidal oxidation can remobilize them through sulfide dissolution. These redox-driven oscillations may expose organisms to episodic metal pulses not captured by single-point concentration measurements, suggesting that the chronic-daily-intake approach used here may underestimate actual exposure at sites influenced by tidal fluctuations. The additive risk models therefore likely underestimate the true health and ecological risk, reinforcing the need for immediate intervention at S1 and S3.

4.6. Spatial Patterns and Source Characterization

The consistent pattern across both pollutant classes—S3 exhibiting the highest contamination, followed by S1, with progressive dilution toward the reference sites—provides strong evidence for petroleum infrastructure as the unified source of contamination. This is corroborated by log-linear distance-decay gradients ($R^2 > 0.85$ for both pollutant classes), strong positive correlations (TPH–Cd r = 0.88; TPH–Ni r = 0.91; all $p < 0.01$; see also Figure 7), consistent diagnostic ratios (CPI $\approx$ 1.0 at contaminated sites; EF > 20 for Cd and Ni), and direct proximity to the infrastructure (S3 on top of a buried pipeline with visible staining; S1 within 200 m of the active flow station). The relatively pristine condition of S5 and S6 (Figure 8) confirms that contamination is localized rather than diffuse, which has positive implications for targeted remediation.

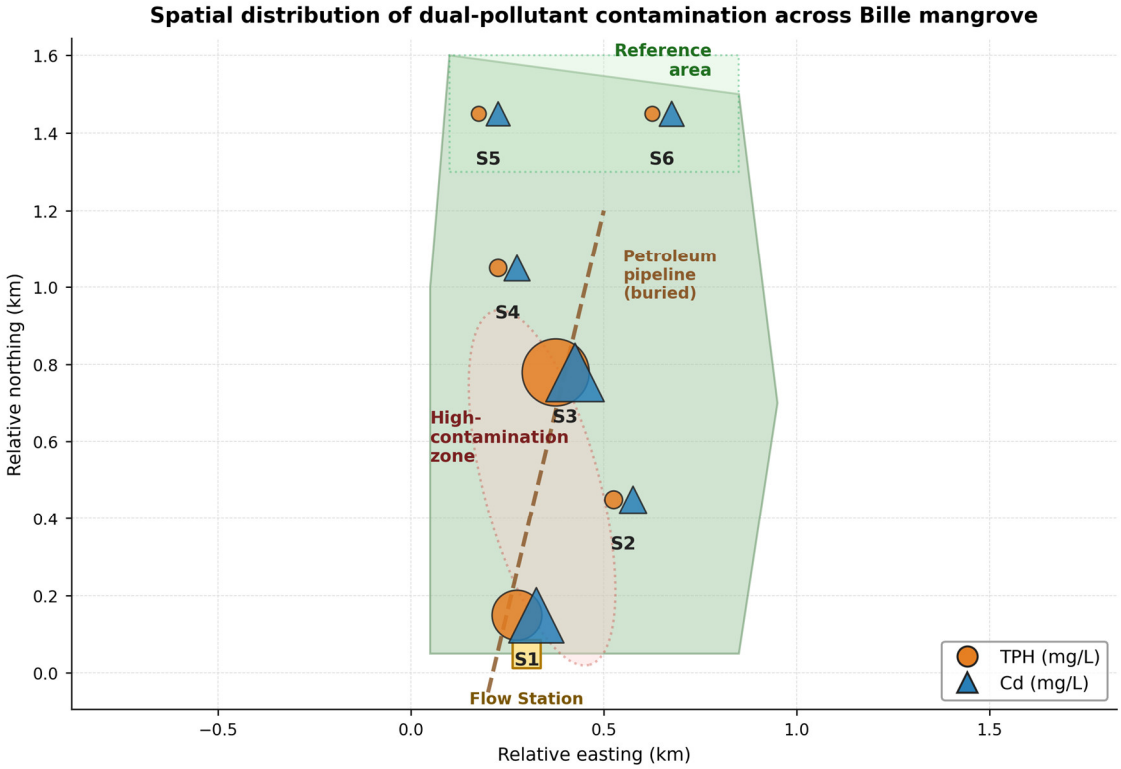


Figure 8. Spatial distribution of dual-pollutant contamination across Bille mangrove showing integrated TPH (orange circles) and cadmium (blue triangles) patterns on relative-distance coordinates. Symbol size scales with pollutant concentration per the legend. The high-contamination zone (light-red ellipse) encompasses S1–S3 near petroleum infrastructure. The yellow square marks the active petroleum-production facility (flow station) with documented spillage history. The dashed brown line indicates the major petroleum pipeline traversing the mangrove (buried section, with visible surface staining at S3). The light-green band represents the reference area (S5, S6) exhibiting minimal contamination. The spatial gradient demonstrates a clear distance-decay relationship between contamination level and petroleum-infrastructure proximity ($R^2 > 0.85$ for both pollutant classes).

4.7. Comparative Assessment with Global Petroleum-Impacted Systems

Contextualizing the Bille contamination within the global landscape (Table 10) reveals important patterns. Bille TPH levels exceed post-Deepwater Horizon Gulf of Mexico measurements by 6–47 times and typical Chinese mangrove systems by 166 times, reflecting chronic petroleum seepage rather than catastrophic spills. Heavy-metal concentrations at Bille are broadly comparable to those of other Niger Delta systems but exhibit substantially higher cadmium and nickel enrichment than global mangrove averages [71].

The critical distinction characterizing Bille as a health emergency is the simultaneous exceedance of carcinogenic-risk thresholds (metal CR > 10^{-4}) by 34–41-fold, non-carcinogenic-risk thresholds (HI > 1) by 20–25-fold, and ecological-risk thresholds (PERI > 600) at petroleum-infrastructure sites, all within a single integrated assessment. This comprehensive risk profile is invisible to single-pollutant assessments and demonstrates the value of the dual-pollutant approach adopted in this study. The integrated risk comparison is presented in Figure 9.

Table 10. Regional comparison of TPH and heavy-metal contamination at Bille mangrove against representative Niger Delta and global mangrove systems. "NR" = not reported in the cited source. Bille TPH is 6–47-fold higher than the post-Deepwater Horizon Gulf of Mexico baseline and approximately 166-fold higher than typical Chinese mangrove sediment, reflecting chronic petroleum seepage from infrastructure rather than discrete catastrophic events.

Location	Matrix	TPH (mg/L or mg/kg)	Metal CR	PERI	Key Metals	Reference
NIGER DELTA REGION						
Bille, Rivers (this study)	Water	0.18–57.66	4.15×10^{-3}	722	Cd, Ni, Pb	This study
Bonny Estuary	Water	17.38–889	NR	PLI 5593	14 metals	Anyanwu [15]
Bodo	Sediment	5000–100,000	NR	NR	TPH, PAHs	Little [52]
Isaka-Bundu	Sediment	NR	NR	691–4447	Cd, Pb, Zn	Chris [10]
Woji Creek	Water	8.42–23.17	NR	NR	TPH, PAHs	Ihunwo [65]
GLOBAL MANGROVE SYSTEMS						
Sundarbans, India	Sediment	1.5–18.6	NR	85–320	Cd, Pb, Cu	[8]
Pearl River, China	Sediment	0.35–2.1	NR	45–180	Cd, Pb, Zn	Review [37]
Gulf of Mexico	Sediment	1.2–8.9	NR	NR	PAHs	Post-DWH [23]
Tampa Bay, USA	Water/Sediment	Trace–1.5	NR	<100	Cu, Pb, Zn	[9]

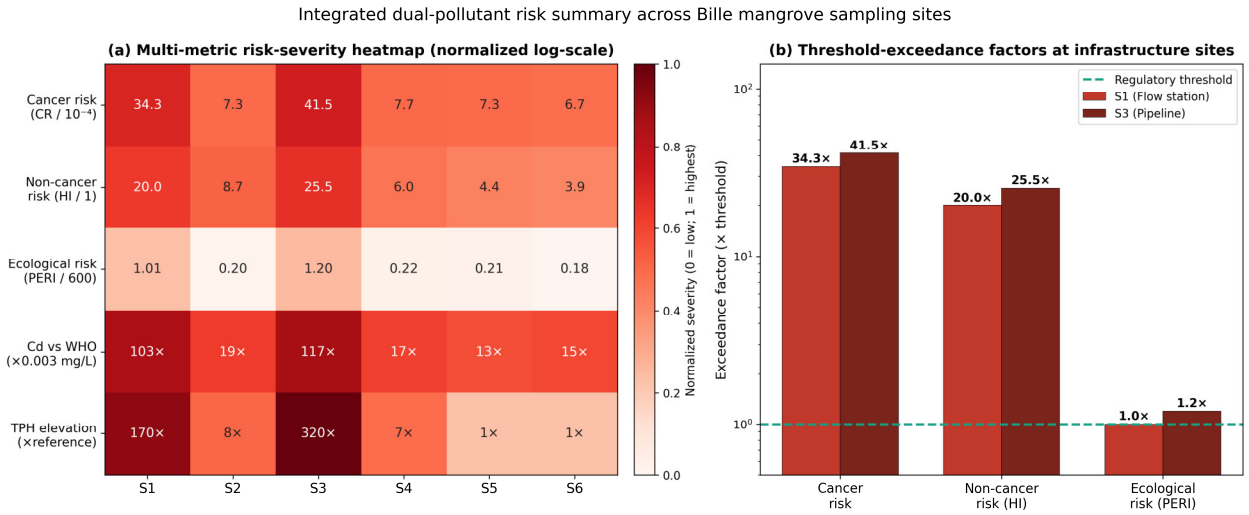


Figure 9. Integrated dual-pollutant risk summary across Bille mangrove sampling sites. Panel (**a**): Multi-metric risk-severity heatmap showing normalized severity (0–1, log-scale color mapping) across five risk dimensions (cancer risk vs. USEPA 10^{-4}; non-cancer risk vs. HI = 1; ecological risk vs. PERI = 600; cadmium concentration vs. WHO 0.003 mg/L; TPH elevation above reference) for all six sites; darker shading indicates higher severity, with raw exceedance values annotated in each cell. S1 and S3 consistently exhibit the highest severity across all metrics. Panel (**b**): Threshold-exceedance factors at S1 (flow station) and S3 (pipeline) expressed as multiples of the respective regulatory thresholds (log scale); S3 shows the highest exceedance for cancer risk (41.5×) and non-carcinogenic risk (25.5×), while S1 shows comparable ecological-risk exceedance (1.0×).

4.8. Environmental Justice and Community-Health Implications

The Bille situation represents a stark case of environmental injustice. Approximately 50,000 residents face heavy-metal carcinogenic risk exceeding the USEPA threshold by 34–41-fold from water exposure alone, while non-carcinogenic risk indicates probable

adverse health effects across all exposure locations. The benefit–risk asymmetry is striking: petroleum extraction generates billions of dollars annually for Rivers State and contributes more than 90% of Nigeria's foreign-exchange earnings, yet the community lacks electricity-grid connection, paved roads, or preferential employment despite hosting the principal petroleum infrastructure and absorbing maximal environmental-health costs [10,60].

The cumulative exposure burden extends beyond the water-column pathway quantified here. Residents are exposed through dietary intake of contaminated fish and shellfish (bioaccumulation factors > 1.5 documented in nearby systems [72]), dermal contact during 4–8 h of daily occupational fishing, inhalation of volatile fractions and particulate-bound metals from gas flaring, and contamination of agricultural crops from petroleum-affected irrigation water. These pathways may increase total health risk by 20–200% beyond water-only calculations. Vulnerable sub-populations face disproportionate risks: children exhibit higher exposure per body weight, pregnant women face developmental toxicity risks (particularly from lead and cadmium), and elderly or immunocompromised individuals have reduced detoxification capacity [44,64].

The health-infrastructure deficit compounds these burdens, as Bille Community lacks cancer-care services, cancer screening, environmental-health surveillance, or biomonitoring capacity. Active litigation (ongoing since 2019) underscores residents' awareness of environmental impacts, and this study provides quantitative evidence supporting community observations. Environmental justice demands remediation, comprehensive health screening, compensation for lost livelihoods, and meaningful participation in environmental decision making.

4.9. Methodological Innovations and Study Limitations

This study advances the field through several methodological contributions. It represents the first simultaneous quantification of TPH and metals in Niger Delta mangrove water within a unified risk framework, whereas previous investigations examined these pollutant classes independently [23,45] or in sediments [25,53] or terrestrial systems [54]. The application of multiple complementary ecological- and health-risk indices across both pollutant classes captures risk dimensions invisible to any single index. The comparative dual-pollutant risk ranking demonstrates that metals drive both carcinogenic and non-carcinogenic risk, providing actionable guidance for remediation. The focus on the water column addresses the primary human-exposure pathway for subsistence communities and enables direct comparison with WHO drinking-water guidelines.

Several limitations constrain the interpretation. The single dry-season sampling campaign cannot capture seasonal variability; Anyanwu et al. [15] documented seasonal differences of 2–5 times in Niger Delta systems, suggesting that annual population-averaged exposures may be 30–60% lower than calculated. BTEX compounds were not separately analyzed; their inclusion as individual carcinogens (particularly benzene) could add 1–10% of the incremental cancer risk attributable to the aromatic TPH fraction. Dietary exposure was not quantified, although subsistence communities consuming 50–150 g/day of mangrove-derived protein may experience 2–3 times greater total metal exposure through bioaccumulation [72]. The additive risk model assumptions neglect potential synergistic interactions between petroleum hydrocarbons and metals, with bioassay studies suggesting a 1.5–3.0-fold increase in toxicity for co-contaminated matrices [58]. The reference sites exhibit detectable metal contamination (HI = 3.9–4.4), representing "minimally affected" rather than pristine conditions, which can cause an underestimation of enrichment actors. Population-average exposure parameters obscure individual variability, likely underestimating the risk for high-exposure subgroups while overestimating it for low-exposure groups.

First, chromium was quantified as total Cr by AAS rather than speciated into Cr(III)/Cr(VI); the carcinogenic-risk calculation conservatively assumes the entirety as Cr(VI), which may overestimate cancer risk if the predominant species in the saline mangrove water is the less toxic Cr(III). Second, the Cd and Ni cancer slope factors of 6.3 and 0.84 (per mg/kg/day) in IRIS [34] are inhalation-derived; their application here to the oral pathway follows the Niger Delta regional convention [44,45,65] but represents a conservative assumption that may inflate oral cancer-risk estimates. Future site investigations at Bille should, therefore, include Cr-speciation analysis (e.g., IC-ICP-MS) and the standardized microbial-toxicity test battery of Strotmann et al. [66] for organism-level confirmation of the calculation-based risk indices reported here.

Despite these limitations, the documented cancer-risk values ($3.43–4.15 \times 10^{-3}$) exceed the USEPA acceptable threshold by 34–41-fold, establishing Bille Community as a critical case study for environmental-health intervention regardless of the uncertainty bounds.

4.10. Management Recommendations and Remediation Prioritization

The integrated risk assessment enables evidence-based remediation prioritization organized in three tiers. The remediation discussion is now tailored to the environmental conditions identified in the study; we therefore expand the prior recommendations into concrete, condition-specific actions below.

Tier 1 (S1 and S3)—immediate intervention. These sites exhibit carcinogenic risk exceeding acceptable thresholds by > 34-fold and non-carcinogenic risk by 20–25-fold, in addition to PERI > 600 and EF $\geq$ 40 for nickel. Three concurrent actions are recommended. **(i) Source control:** Emergency pipeline-integrity assessment and repair at S3, including in-line inspection (smart-pigging) and replacement of corroded sections; upgrade of flow-station produced-water treatment at S1 to incorporate a cadmium-selective ion-exchange polisher (sulfhydryl-functionalized resins or zeolite-based sorbents) prior to discharge [73]. **(ii) Active in situ remediation:** Given the elevated TOC (9.3–11.3%) and tidal influence at S1 and S3, deployment of in situ stabilization using biochar amendment (rice-husk biochar at 2–5% w/w has been shown to reduce Cd bioavailability by 60–80% in oil-impacted Niger Delta sediments [73]) is preferred over excavation, which would mobilize sediment-bound metals into the water column. Phytoremediation using metal-tolerant *Rhizophora racemosa* complemented by *Avicennia germinans* (which exhibits superior cadmium-translocation control via salt-gland exclusion [8,74]) should be initiated in flanking zones to provide longer-term rhizosphere-mediated metal immobilization. **(iii) Community-health response:** Biomonitoring (urinary cadmium and blood lead) for residents within 500 m of S1 and S3, prioritizing children and pregnant women; provision of safe alternative drinking water through deeper-borehole drilling beyond the contaminated horizon; and a community-health registry to track long-term outcomes. Implementation timeline: Source-control measures within 0–6 months; active remediation within 1–3 years; biomonitoring to begin within 3 months and continue indefinitely.

Tier 2 (S2 and S4)—active monitoring with contingent intervention. These sites demonstrate elevated but not extreme risk (HI = 6.0–8.7; CR $\approx 7 \times 10^{-4}$). Recommended actions: (i) quarterly water and sediment sampling for Cd, Ni, Pb, Cr, and TPH for at least 24 months; (ii) biomonitoring using sentinel species (mangrove oysters, Crassostrea gasar, and periwinkles, Tympanotonus fuscatus) to verify whether bioaccumulation is keeping pace with water-column concentrations; (iii) intervention to be escalated to Tier 1 if any two consecutive quarters show > 25% upward concentration trend or if biota tissue Cd exceeds 1 mg/kg dry weight [72].

Tier 3 (S5 and S6)—reference protection and baseline maintenance. These sites serve as essential reference locations and must be protected. Recommended actions: (i) For-

mal protective zoning with a 1 km exclusion buffer for new petroleum infrastructure; (ii) annual baseline monitoring at low-density sampling (one campaign per dry season); (iii) restoration trials in the old artisanal bunkering area (S6) using complementary microbial bioremediation strategies (cow-dung biostimulation has demonstrated 23% additional TPH removal relative to fertilizer-only controls in Niger Delta mangrove sediments [75]); and (iv) sentinel hydrocarbon-utilizing bacterial assessment to verify the natural-attenuation capacity has been restored [10,26].

Regional policy reforms. These site-level actions must be accompanied by regional policy reforms. (i) Mandate simultaneous TPH and heavy-metal assessment for all petroleum operations in mangrove zones; (ii) update EGASPIN to include water-specific and mangrove-specific thresholds for Cd, Cr, Pb, Ni, and Zn (current EGASPIN is sediment-focused); (iii) adopt metal cancer risk $>10^{-4}$ as a mandatory remediation trigger; (iv) establish health registries for petroleum-impacted communities; and (v) require benefit-sharing mechanisms that ensure proportional compensation and health services for impacted communities. Recent reviews of remediation technology in the Niger Delta [76,77] support the joint deployment of organoclay-based reactive core materials for sediment, permeable reactive barriers for groundwater, and bioremediation for surface soils as the most cost-effective integrated strategy for the region.

5. Conclusions

This study provides the first comprehensive, integrated assessment of total petroleum hydrocarbons (TPH) and metals in mangrove water from the Niger Delta, revealing a significant cumulative health and ecological risk profile in Bille Community. Four principal conclusions emerge.

First, metals were identified as the dominant risk driver across all assessment dimensions. Carcinogenic risk from metals reached 4.15×10^{-3} at Site 3, exceeding the USEPA acceptable threshold by 41-fold, with cadmium contributing 86–88% of total metal cancer risk. Non-carcinogenic risk was extreme, with HI values of 20.03–25.51 at petroleum-infrastructure sites, driven primarily by cadmium, lead, and nickel. All six sites exhibited HI values exceeding unity, with cadmium and nickel demonstrating extreme enrichment (EF = 28.6–77.6; I_{geo} = 2.95–4.39) and concentrations exceeding WHO drinking-water guidelines by 17–117-fold.

Second, TPH concentrations confirmed widespread petroleum contamination, with a 320-fold elevation at Site 3 relative to reference sites, but the health risk from TPH in the water pathway was minimal compared with metals, because TPH lacks established cancer slope factors, and its fraction-based non-carcinogenic risk (HQ) remained below unity. Nevertheless, TPH serves as an essential indicator of the petroleum-contamination source that delivers the co-occurring toxic metals.

Third, the ecological-risk assessment documented very high conditions at petroleum-infrastructure sites, with heavy-metal PERI values of 603–722 driven by cadmium (Er = 310–350) and nickel (Er = 75–140). Source apportionment through CPI values approaching unity, enrichment factors exceeding 20, and strong TPH–metal correlations ($r > 0.88$) conclusively implicated petroleum operations as the primary contamination source.

Fourth, the consistent spatial gradient across both pollutant classes, combined with diagnostic source indicators, enables targeted remediation prioritized at Sites 1 and 3, where both carcinogenic and non-carcinogenic risk thresholds are exceeded by the greatest margins. Site-specific remediation strategies suited to the conditions documented in this study are detailed in Section 4.10 and summarized here as a three-tier framework: immediate intervention at S1 and S3 (Tier 1) combining pipeline-integrity assessment, biochar-amended

in situ stabilization, *Rhizophora*/*Avicennia* phytoremediation, and biomonitoring of exposed residents; active monitoring with biota-based triggers at S2 and S4 (Tier 2); and reference-site protection with cow-dung biostimulation of the bunkering area at S6 (Tier 3) [73,75,76].

This work addresses a critical gap by providing the first simultaneous quantification of TPH and metals within a comprehensive risk framework for Niger Delta mangrove water, allowing the identification of metals as the dominant risk driver and the development of scientifically defensible remediation priorities. Immediate intervention is required at Sites 1 and 3, and regional policy reforms should mandate integrated dual-pollutant monitoring and metal cancer-risk-based remediation triggers. Future research should pursue long-term seasonal monitoring, bioaccumulation and dietary-exposure studies, human biomonitoring for cadmium and lead, and evaluation of synergistic toxicological interactions between TPH and metals under field conditions.

Comparative Regional Context; For ease of reference, Table 10 summarizes how the Bille findings compare with representative Niger Delta and global mangrove studies.

Author Contributions: O.G.O. designed the study, conducted field sampling and laboratory analysis, performed data analysis, and drafted the manuscript. V.V.P. supervised the research and provided careful and critical review of the manuscript. All authors have read and agreed to the published version of the manuscript.

Funding: This research was supported by the RUDN University Scientific Projects Grant System. Project No: 202789-2-000.

Data Availability Statement: All data generated or analyzed during this study are included in this article. Raw analytical data, including GC-FID chromatograms and AAS measurement records, are available from the corresponding author upon reasonable request.

Acknowledgments: The authors acknowledge Bille Community leadership for granting access to sampling sites and providing logistical support during the field campaigns. The authors also thank the three anonymous reviewers and the editor whose comments and suggestions substantially improved the methodological rigor and presentation of this manuscript.

Conflicts of Interest: The authors declare no conflicts of interest.

References

1. Duke, N.C.; Meynecke, J.O.; Dittmann, S.; Ellison, A.M.; Anger, K.; Berger, U.; Cannicci, S.; Diele, K.; Ewel, K.C.; Field, C.D.; et al. A world without mangroves? *Science* **2007**, *317*, 41–42. [CrossRef]
2. Valiela, I.; Bowen, J.L.; York, J.K. Mangrove forests: One of the world's threatened major tropical environments. *BioScience* **2001**, *51*, 807–815. [CrossRef]
3. Spalding, M.; Kainuma, M.; Collins, L. *World Atlas of Mangroves*; Earthscan: London, UK; Washington, DC, USA, 2010.
4. Barbier, E.B.; Hacker, S.D.; Kennedy, C.; Koch, E.W.; Stier, A.C.; Silliman, B.R. The value of estuarine and coastal ecosystem services. *Ecol. Monogr.* **2011**, *81*, 169–193. [CrossRef]
5. Burns, K.A.; Garrity, S.D.; Levings, S.C. How many years until mangrove ecosystems recover from catastrophic oil spills? *Mar. Pollut. Bull.* **1993**, *26*, 239–248. [CrossRef]
6. Ke, L.; Wong, T.W.Y.; Wong, Y.S.; Tam, N.F.Y. Fate of polycyclic aromatic hydrocarbon (PAH) contamination in a mangrove swamp in Hong Kong following an oil spill. *Mar. Pollut. Bull.* **2002**, *45*, 339–347. [CrossRef] [PubMed]
7. Holguín, G.; Vazquez, P.; Bashan, Y. The role of sediment microorganisms in the productivity, conservation, and rehabilitation of mangrove ecosystems: An overview. *Biol. Fertil. Soils* **2001**, *33*, 265–278. [CrossRef]
8. MacFarlane, G.R.; Koller, C.E.; Blomberg, S.P. Accumulation and partitioning of metals in mangroves: A synthesis of field-based studies. *Chemosphere* **2007**, *69*, 1454–1464. [CrossRef] [PubMed]
9. Lewis, M.A.; Russell, M.J. Contaminant profiles for surface water, sediment, flora and fauna associated with the mangrove fringe along middle and lower eastern Tampa Bay. *Mar. Pollut. Bull.* **2015**, *95*, 273–282. [CrossRef] [PubMed]
10. Chris, O.A.; Anyanwu, B.O. Heavy-metal contamination and ecological-risk assessment of tidal mangrove water and sediments of the Niger Delta: An integrated index-based study. *Environ. Monit. Assess.* **2023**, *195*, 1217. [CrossRef] [PubMed]
11. Speight, J.G. *The Chemistry and Technology of Petroleum*; CRC Press: Boca Raton, FL, USA, 2016.

12. Wang, Z.; Fingas, M.; Page, D.S. Oil spill identification. *J. Chromatogr. A* **1999**, *843*, 369–411. [CrossRef]
13. Kadafa, A.A. Oil exploration and spillage in the Niger Delta of Nigeria. *Civ. Environ. Res.* **2012**, *2*, 38–51.
14. Ordinioha, B.; Brisibe, S. The human health implications of crude oil spills in the Niger Delta, Nigeria: An interpretation of published studies. *Niger. Med. J.* **2013**, *54*, 10–16. [CrossRef] [PubMed]
15. Anyanwu, B.O.; Ezejiofor, A.N.; Igweze, Z.N.; Orisakwe, O.E. Pollution of the Niger Delta with total petroleum hydrocarbons, metals and nutrients in relation to seasonal dynamics. *Sci. Rep.* **2023**, *13*, 14079. [CrossRef] [PubMed]
16. Venosa, A.D.; Zhu, X. Biodegradation of crude oil contaminating marine shorelines and freshwater wetlands. *Spill Sci. Technol. Bull.* **2003**, *8*, 163–178. [CrossRef]
17. Peters, K.E.; Walters, C.C.; Moldowan, J.M. *The Biomarker Guide: Volume 2, Biomarkers and Isotopes in Petroleum Systems and Earth History*; Cambridge University Press: Cambridge, UK, 2005. [CrossRef]
18. Zakaria, M.P.; Takada, H.; Tsutsumi, S.; Ohno, K.; Yamada, J.; Kouno, E.; Kumata, H. Distribution of polycyclic aromatic hydrocarbons (PAHs) in rivers and estuaries in Malaysia: A widespread input of petrogenic PAHs. *Environ. Sci. Technol.* **2002**, *36*, 1907–1918. [CrossRef] [PubMed]
19. Redman, A.D.; Parkerton, T.F.; McGrath, J.A.; Di Toro, D.M. PETROTOX: An aquatic toxicity model for petroleum substances. *Environ. Toxicol. Chem.* **2012**, *31*, 2498–2506. [CrossRef] [PubMed]
20. Incardona, J.P.; Scholz, N.L. The influence of heart developmental anatomy on cardiotoxicity-based adverse outcome pathways in fish. *Aquat. Toxicol.* **2016**, *177*, 492–504. [CrossRef] [PubMed]
21. Bosch, C.; Gravina, B.; Laffont, R.; Sala, R. BTEX contamination in urban soils. *Environ. Pollut.* **2021**, *271*, 116337. [CrossRef] [PubMed]
22. Edwards, D.A.; Andriot, M.D.; Amoruso, M.A.; Tummey, A.C.; Bevan, C.J.; Tveit, A.; Hayes, L.A.; Youngren, S.H.; Nakles, D.V. *Total Petroleum Hydrocarbon Criteria Working Group, Development of Fraction-Specific Reference Doses (RfDs) and Reference Concentrations (RfCs) for Total Petroleum Hydrocarbons (TPH)*; Amherst Scientific Publishers: Amherst, MA, USA, 1997.
23. Barron, M.G.; Vivian, D.N.; Heintz, R.A.; Yim, U.H. Long-Term Ecological Impacts from Oil Spills: Comparison of *Exxon Valdez*, *Hebei Spirit*, and Deepwater Horizon. *Environ. Sci. Technol.* **2020**, *54*, 6456–6467. [CrossRef] [PubMed]
24. Department of Petroleum Resources. *Environmental Guidelines and Standards for the Petroleum Industry in Nigeria (EGASPIN)*, 3rd ed.; Department of Petroleum Resources: Lagos, Nigeria, 2018. Available online: https://www.scirp.org/reference/referencespapers?referenceid=3602333 (accessed on 20 April 2026).
25. Little, D.I.; Bullimore, B.; Galperin, Y.; Macadam, I.; Mulligan, K.A. A study of the relationship between soil total petroleum hydrocarbon concentration and the abundance of two earthworm species in crude oil-contaminated soils. *Appl. Soil Ecol.* **2018**, *132*, 125–131. [CrossRef]
26. Aransiola, F.T.; Aransiola, T.A.; Adigun, M.O.; Abioye, O.P.; Oyewole, J.O.; Ojo, S. Microbial communities and bioremediation potential in the Niger Delta mangrove sediments contaminated with petroleum hydrocarbons: A meta-analytic review. *Microbiol. Res.* **2024**, *280*, 127571. [CrossRef] [PubMed]
27. Ketil, H. Bioaccumulation in Marine Organisms: Effect of Contaminants from Oil Well Produced Water. *J. Exp. Mar. Biol. Ecol.* **2003**, *287*, 135–137. [CrossRef]
28. Otton, J.K. *NORM in Petroleum Production*; Fact Sheet FS-142-97; USGS: Reston, VA, USA, 1997.
29. Tchounwou, P.B.; Yedjou, C.G.; Patlolla, A.K.; Sutton, D.J. Metal toxicity and the environment. In *Experientia Supplementum*; Springer: Berlin/Heidelberg, Germany, 2012; Volume 101, pp. 133–164. [CrossRef] [PubMed]
30. Filby, R.H. *Origin and Nature of Trace Element Species in Crude Oils, Bitumens and Kerogens: Implications for Correlation and Other Geochemical Studies*; Special Publications; Geological Society: London, UK, 1987; Volume 40, pp. 203–219. [CrossRef]
31. International Agency for Research on Cancer. Arsenic, metals, fibres, and dusts. In *IARC Monographs on the Evaluation of Carcinogenic Risks to Humans*; IARC Press: Lyon, France, 2012; Volume 100C.
32. US Environmental Protection Agency. *Risk Assessment Guidance for Superfund: Volume III—Part A, Process for Conducting Probabilistic Risk Assessment*; US Environmental Protection Agency: Washington, DC, USA, 2001.
33. Agency for Toxic Substances and Disease Registry. *Public Health Assessment Guidance Manual (Update)*; Agency for Toxic Substances and Disease Registry: Atlanta, GA, USA, 2005.
34. US Environmental Protection Agency. *Integrated Risk Information System (IRIS) Chemical Assessment Summary: Cadmium, Chromium(VI), Lead and Inorganic Pb Compounds, Nickel Soluble Salts*; USEPA Office of Research and Development: Washington, DC, USA, 2025. Available online: https://iris.epa.gov (accessed on 20 April 2026).
35. California Office of Environmental Health Hazard Assessment. *Public Health Goals (PHGs) for Chemicals in Drinking Water: Cadmium, Chromium(VI), Lead, and Nickel—Technical Support Documents*; California Office of Environmental Health Hazard Assessment: Sacramento, CA, USA, 2024. Available online: https://oehha.ca.gov/sites/default/files/media/downloads/water/chemicals/122206cadmiumphg.pdf (accessed on 20 April 2026).
36. Müller, G. Index of geoaccumulation in sediments of the Rhine River. *Geojournal* **1969**, *2*, 108–118.

37. Tomlinson, D.L.; Wilson, J.G.; Harris, C.R.; Jeffrey, D.W. Problems in the assessment of heavy-metal levels in estuaries and the formation of a pollution index. *Helgoländer Meeresunters.* **1980**, *33*, 566–575. [CrossRef]
38. Sutherland, R.A. Bed sediment-associated trace metals in an urban stream, Oahu, Hawaii. *Environ. Geol.* **2000**, *39*, 611–627. [CrossRef]
39. Kowalska, J.B.; Mazurek, R.; Gałsiorék, M.; Zaleski, T. Pollution indices as useful tools for the comprehensive evaluation of the degree of soil contamination—A review. *Environ. Geochem. Health* **2018**, *40*, 2395–2420. [CrossRef] [PubMed]
40. Håkanson, L. An ecological risk index for aquatic pollution control: A sedimentological approach. *Water Res.* **1980**, *14*, 975–1001. [CrossRef]
41. Islam, M.S.; Ahmed, M.K.; Raknuzzaman, M.; Habibullah-Al-Mamun, M.; Islam, M.K. Metal pollution in surface water and sediment: A preliminary assessment of an urban river in a developing country. *Ecol. Indic.* **2015**, *48*, 282–291. [CrossRef]
42. Adamu, C.I.; Nganje, T.N.; Edet, A. Metal contamination and health risk assessment associated with abandoned barite mines in Cross River State, southeastern Nigeria, Environmental Nanotechnology. *Monit. Manag.* **2015**, *3*, 10–21.
43. Yang, Z.; Wang, Y.; Shen, Z.; Niu, J.; Tang, Z. Distribution and speciation of metals in sediments from the mainstream, tributaries, and lakes of the Yangtze River catchment of Wuhan, China. *J. Hazard. Mater.* **2009**, *166*, 1186–1194. [CrossRef] [PubMed]
44. Benjamin, O.D.; Adewole, M.G.; Adewale, M.T.; Olatunbosun, S.S.; Moses, O.D. Carcinogenic and non-carcinogenic health risk assessment of heavy metals in water from selected oil pollution-prone communities in the Niger delta region. *J. Trace Elem. Miner.* **2025**, *14*, 100266. [CrossRef]
45. Effiong, J.U.; Friday, M.C.; Greogry, A.U. Ecological and Health Risk Assessment of Trace Metals in Waters from North-West Zone of Akwa Ibom State, Nigeria. *Pollution* **2023**, *9*, 271–285.
46. Ihinmikaiye, S.O.; Ojo, V.I. Ecological Risk Assessment of Heavy Metals in Nembe Mangrove Forest Sediments, Bayelsa State. *Greener J. Biol. Sci.* **2025**, *15*, 51–59. [CrossRef]
47. United Nations Environment Programme. *Environmental Assessment of Ogoniland*; United Nations Environment Programme: Nairobi, Kenya, 2006.
48. Kadafa, A.A.; Zakaria, M.P.; Othman, F. Oil spillage and pollution in Nigeria: Organizational management and institutional framework. *J. Environ. Earth Sci.* **2012**, *2*, 22–30.
49. International, A. *Nigeria: Petroleum, Pollution and Poverty in the Niger Delta*; Amnesty International: London, UK, 2015.
50. Aghalino, S.O. Corporate response to environmental deterioration in the oil bearing area of the Niger Delta, Nigeria, 1984–2000. *J. Sustain. Dev. Afr.* **2009**, *11*, 281–294.
51. Powell, C.B. A preliminary assessment of the status of mangrove ecosystems in the Niger Delta, Nigeria. *Mangrove Ecosyst. Occas. Pap.* **1985**, *5*, 1–30.
52. Linden, O.; Palsson, J. Oil contamination in Ogoniland, Niger Delta. *Ambio* **2013**, *42*, 685–701. [CrossRef] [PubMed]
53. Iwegbue, C.M.A.; Nwajei, G.E.; Arimoro, F.O.; Eguavoen, O.I. Characteristic levels, spatial distribution and ecological risk assessment of polycyclic aromatic hydrocarbons in soils of an urban environment in the Niger Delta, Nigeria. *Environ. Geochem. Health* **2019**, *41*, 1373–1387. [CrossRef]
54. Nwaichi, E.O.; Wegwu, M.O.; Nwosu, U.L. Distribution of selected carcinogenic hydrocarbon and metals in an oil-polluted agricultural zone. *Environ. Monit. Assess.* **2014**, *186*, 8697–8706. [CrossRef] [PubMed]
55. Carpenter, D.O.; Arcaro, K.; Spink, D.C. Understanding the human health effects of chemical mixtures. *Environ. Health Perspect.* **2002**, *110*, 25–42. [CrossRef] [PubMed]
56. Loureiro, S.; Svendsen, C.; Ferreira, A.L.G.; Pinheiro, C.; Ribeiro, F.; Soares, A.M.V.M. Toxicity of three binary mixtures to Daphnia magna: Comparing chemical modes of action and deviations from conceptual models. *Environ. Toxicol. Chem.* **2010**, *29*, 1716–1726. [CrossRef] [PubMed]
57. Weng, L.; Temminghoff, E.J.M.; Lofts, S.; Tipping, E.; Van Riemsdijk, W.H. Complexation with dissolved organic matter and solubility control of metals in a sandy soil. *Environ. Sci. Technol.* **2002**, *36*, 4804–4810. [CrossRef] [PubMed]
58. Khudur, L.S.; Shahsavari, E.; Webster, P.G.; Nugegoda, E.; Ball, A.S. Implications of co-contamination with aged metals and total petroleum hydrocarbons on natural attenuation and ecotoxicity in Australian soils. *Environ. Pollut.* **2019**, *243*, 94–102. [CrossRef] [PubMed]
59. Neff, J.M.; Lee, K.; DeBlois, E.M. Produced water: Overview of composition, fates, and effects. In *Produced Water*; Springer: Berlin/Heidelberg, Germany, 2011; pp. 3–54. [CrossRef]
60. Onyena, A.P.; Sam, K. A review of the threat of oil exploitation to mangrove ecosystem: Insights from Niger Delta, Nigeria. *Glob. Ecol. Conserv.* **2020**, *22*, e00961. [CrossRef]
61. Anejionu, O.C.D.; Blackburn, G.A.; Whyatt, J.D. Detecting gas flares and estimating flaring volumes at individual flow stations using MODIS data. *Remote Sens. Environ.* **2015**, *158*, 81–94. [CrossRef]
62. US Environmental Protection Agency. Method 8015C (Revision 3): Nonhalogenated organics by gas chromatography. In *SW-846 Compendium*; US Environmental Protection Agency: Washington, DC, USA, 2007. Available online: https://www.epa.gov/hw-sw846 (accessed on 20 April 2026).

63. Interstate Technology and Regulatory Council. *TPH Risk Evaluation at Petroleum-Contaminated Sites*; Interstate Technology and Regulatory Council: Washington, DC, USA, 2018. Available online: https://tphrisk-1.itrcweb.org (accessed on 20 April 2026).
64. US Environmental Protection Agency. *Exposure Factors Handbook: 2011 Edition (Final)*; USEPA Office of Research and Development: Washington, DC, USA, 2011. Available online: https://www.epa.gov/expobox/exposure-factors-handbook-2011-edition (accessed on 20 April 2026).
65. Ihunwo, O.C.; Aiwansoba, A.B.; Osuji, G.N.; Akajiaku, L.C. Ecological and human health risk assessment of total petroleum hydrocarbons in surface water and sediment from Woji Creek in the Niger Delta estuary of Rivers State, Nigeria. *Heliyon* **2021**, *7*, e07689. [CrossRef] [PubMed]
66. Strotmann, T.G.; Schaffer, A.; Bahnemann, B.; Otieno, B.P.P.; Walker, T.R.; Lara-Martín, K.; Hesterberg, M. OECD/ISO standardized testing of environmental fate and toxicity of chemicals: A critical review of methods, applications, and limitations. *Appl. Microbiol. Biotechnol.* **2024**, *108*, 348. [CrossRef] [PubMed]
67. *ISO 11348-1:2007*; Water Quality—Determination of the Inhibitory Effect of Water Samples on the Light Emission of *Vibrio fischeri* (Luminescent BACTERIA test)—Part 1: Method Using Freshly Prepared Bacteria. ISO: Geneva, Switzerland, 2007.
68. *ISO 9377-2:2000*; Water Quality: Determination of Hydrocarbon Oil Index. Part 2: Method Using Solvent Extraction and Gas Chromatography. International Organization for Standardization: Geneva, Switzerland, 2000.
69. American Public Health Association. *American Water Works Association, Water Environment Federation, Standard Methods for the Examination of Water and Wastewater*, 23rd ed.; American Public Health Association: Washington, DC, USA, 2017.
70. Ehiemere, C.C.; Iorhemen, R.C.; Akpan, A.C. Distribution and ecological-risk assessment of metals in surface water and sediments from petroleum-impacted mangrove creeks of the Niger Delta, Nigeria. *Environ. Sci. Pollut. Res.* **2024**, *31*, 8453–8472. [CrossRef] [PubMed]
71. Wu, Y.; Xi, B.; Su, R.; Tan, X.; Liu, D.; Xiao, W.; Hu, Q. Ecological-risk evaluation of metals in mangrove sediments based on improved Nemerow index and self-organizing-map clustering: Global synthesis and policy implications. *Environ. Pollut.* **2024**, *341*, 122972. [CrossRef] [PubMed]
72. Saunders, D.; Juan, C.C.; Erich, R.G.; Ogonnaya, I.; Kabari, V.; Nenibarini, Z.; Matthijs, B. Analysis of polycyclic aromatic hydrocarbons (PAHs) in surface sediments and edible aquatic species in an oil-contaminated mangrove ecosystem in Bodo, Niger Delta, Nigeria: Bioaccumulation and human health risk assessment. *Sci. Total Environ.* **2022**, *832*, 154802. [CrossRef] [PubMed]
73. Akagbue, A.C.; Onuoha, F.C.; Otabor, J.K. Biochar amendment for immobilization of cadmium and lead in oil-impacted Niger Delta sediments: A column-based study. *J. Environ. Chem. Eng.* **2024**, *12*, 113521. [CrossRef]
74. Mohajeri, M.; Lashkaripour, B.; Kalantari, S.; Behzad, M. Phytoremediation of cadmium- and lead-contaminated mangrove wetlands using Rhizophora and Avicennia species: Mechanisms and field performance. *Plant Soil* **2023**, *491*, 357–378. [CrossRef]
75. Sam, K.; Onyena, A.P.; Erakhrumen, T. Cow-dung biostimulation enhances total petroleum hydrocarbon attenuation in artisanal-refining-impacted Niger Delta mangrove sediments. *J. Hazard. Mater. Adv.* **2024**, *13*, 100408. [CrossRef]
76. Oyebamiji, O.E.; Oguntoke, O.O.; Olukosi, S.; Iyanda, M.O. A review of remediation technologies for hydrocarbon and heavy-metal contamination in Niger Delta: Status, gaps, and integration prospects. *Environ. Geochem. Health* **2024**, *46*, 295. [CrossRef] [PubMed]
77. Shijie, W.; Xiang, W. Bioremediation of Petroleum contaminated soils collected all around China: The extensive application and the microbial mechanism. *Pet. Sci. Technol.* **2018**, *36*, 974–980. [CrossRef]

Disclaimer/Publisher's Note: The statements, opinions and data contained in all publications are solely those of the individual author(s) and contributor(s) and not of MDPI and/or the editor(s). MDPI and/or the editor(s) disclaim responsibility for any injury to people or property resulting from any ideas, methods, instructions or products referred to in the content.